bioRxiv preprint doi: https://doi.org/10.1101/159376; this version posted July 4, 2017. The copyright holder for this preprint (which was not certified by peer review) is the author/funder, who has granted bioRxiv a license to display the preprint in perpetuity. It is made available under aCC-BY 4.0 International license.

1 # Context-dependent deposition and regulation of mRNAs in P-bodies
2
3
4 Congwei Wang[1], Fabian Schmich[2,3], Julie Weidner[1], Niko Beerenwinkel[2,3] and Anne Spang[1]
5 [1]Growth & Development, Biozentrum, University of Basel, Klingelbergstrasse 70, CH-4056 Basel,
6 Switzerland
7 [2]Department of Biosystems Science and Engineering, ETH Zürich, Mattenstrasse 26, CH-4058
8 Basel, Switzerland
9 [3]SIB, Swiss Institute of Bioinformatics, Mattenstrasse 26, CH-4058 Basel, Switzerland
10
11
12
13 Address of correspondence:
14 Anne Spang
15 Biozentrum
16 University of Basel
17 Klingelbergstrasse 70
18 4056 Basel
19 Switzerland
20 Phone: + 41 61 267 2380
21 FAX: + 41 61 267 0759
22 email: anne.spang@unibas.ch
23

bioRxiv preprint doi: https://doi.org/10.1101/159376; this version posted July 4, 2017. The copyright holder for this preprint (which was not certified by peer review) is the author/funder, who has granted bioRxiv a license to display the preprint in perpetuity. It is made available under aCC-BY 4.0 International license.

24 **Abstract**

25

26 Cells respond to stress by remodeling their transcriptome through transcription and degradation.
27 Xrn1p-dependent degradation in P-bodies is the most prevalent pathway. Yet, P-bodies may
28 facilitate not only decay but also act as storage compartment. However, which and how mRNAs
29 are selected into different degradation pathways and what determines the fate of any given mRNA
30 in P-bodies remain largely unknown. We devised a new method to identify both common and
31 stress-specific mRNA subsets associated with P-bodies. mRNAs targeted for degradation to P-
32 bodies, decayed with different kinetics. Moreover, the localization of a specific set of mRNAs to
33 P-bodies under glucose deprivation was obligatory to prevent decay. Depending on its client
34 mRNA, the RNA binding protein Puf5p either promoted or inhibited decay. The Puf5p-dependent
35 storage of a subset of mRNAs in P-bodies under glucose starvation may be beneficial with respect
36 to chronological lifespan.

37

38

bioRxiv preprint doi: https://doi.org/10.1101/159376; this version posted July 4, 2017. The copyright holder for this preprint (which was not certified by peer review) is the author/funder, who has granted bioRxiv a license to display the preprint in perpetuity. It is made available under aCC-BY 4.0 International license.

39 **Introduction**

40

41 Cells are often subjected to environmental fluctuations, such as nutrient deficiency, osmotic shock
42 and temperature change. Therefore, cells have evolved a variety of cellular mechanisms to adapt
43 and survive under those conditions, which are generally referred to as stress responses (Mager
44 and Ferreira, 1993). Regulation of transport, translation and stability of mRNAs are among the
45 first acute responses contributing to the rapid adjustment of the proteome. In response to stress,
46 protein synthesis is globally attenuated, but a subset of mRNAs, necessary to cope with the stress,
47 is still subject to efficient translation (Ashe et al., 2000). Non-translating mRNAs are mostly
48 deposited into processing bodies (P-bodies) and stress granules (SGs), which are two types of
49 ribonucleoprotein particles (RNP), conserved from yeast to mammals. As the formation of both
50 granules is induced under diverse stress conditions and a number of components appears to be
51 shared, their precise role in stress response is still a matter of debate (Kulkarni et al., 2010;
52 Mitchell et al., 2013). While P-bodies and SGs both participate in repression of translation and
53 mRNA storage, P-bodies represent also a main site for mRNA degradation through the 5'-
54 decapping-dependent pathway, the 5'-3' exonuclease Xrn1p and transport (Decker and Parker,
55 2012) (Davidson et al., 2016). In addition to the decay in P-bodies, a 3'-5' exonucleolytic pathway
56 exists (Anderson and Parker, 1998). More recently a co-translational RNA decay pathway has
57 been discovered, which responds to ribosome transit rates (Pelechano et al., 2015; Sweet et al.,
58 2012). Interestingly, some of the P-body components such as the helicase Dhh1p and the
59 exonuclease Xrn1p also act in the co-translational pathway. Moreover, other P-body components
60 such as the decapping activator Dcp2p have been found to associate with polysomes (Weidner
61 et al., 2014). How and which mRNAs are selected into the different pathways, in particular under
62 stress, remains elusive, partly because unbiased methods to identify RNA species are still not
63 widely used. Here, we devised a novel method to identify RNA species in ribonucleotide particles
64 (RNPs), in particular P-bodies.

bioRxiv preprint doi: https://doi.org/10.1101/159376; this version posted July 4, 2017. The copyright holder for this preprint (which was not certified by peer review) is the author/funder, who has granted bioRxiv a license to display the preprint in perpetuity. It is made available under aCC-BY 4.0 International license.

65 The protein composition of P-bodies has been extensively studied in both yeast and
66 metazoan (Kulkarni et al., 2010), yet, numerous auxiliary and transient components are still being
67 discovered (Hey et al., 2012; Ling et al., 2014; Weidner et al., 2014), suggesting a tight regulation
68 of the RNA inventory and fate. However, very little is known about the regulation of mRNA fate in
69 P-bodies. To date, the RNA inventory in P-bodies under particular stress remains unclear, and in
70 yeast only a handful of mRNAs have been confirmed to localize to P-bodies (Brengues et al.,
71 2005; Cai and Futcher, 2013; Lavut and Raveh, 2012). Several studies have proposed P-bodies
72 to act not only as decay compartments but also to store and later release RNAs back into the
73 translation pool, particularly upon stress removal. This notion is primarily supported by an
74 observed dynamic equilibrium of mRNA localization between polysomes and P-bodies (Brengues
75 et al., 2005; Kedersha et al., 2005; Teixeira et al., 2005). Recently this model has been challenged
76 and it was proposed that Xrn1p-dependent decay might occur outside P-bodies (Sweet et al.,
77 2012), which is supported by findings that the 5' decapping machinery is present at membrane-
78 associated polysomes under non stress conditions (Huch et al., 2016; Weidner et al., 2014). Still,
79 a prevailing hypothesis in the field is that specific mRNAs preferentially accumulate in P-bodies
80 under different stresses promoting cell adaption and survival (Decker and Parker, 2012). In
81 support of this concept, the number, morphology and half-life of P-bodies vary depending on the
82 particular stress. For example, under glucose starvation only a few, large, long-lived P-bodies are
83 observed, whereas Ca^{2+} stress produces numerous, small P-bodies that disappear within 30 to
84 45 min after the initial induction (Kilchert et al., 2010). Lacking a global picture of mRNA species
85 in P-bodies greatly hinders the study of the functional role of P-bodies in mRNA turnover and
86 stress response.

87 A major obstacle in the universal identification of mRNAs present in P-bodies is that at
88 least a portion of the transcripts are likely engaged in deadenylation or degradation, and, hence,
89 commonly used oligo(dT) purification provides an incomplete and biased picture of mRNAs
90 present in P-bodies. We overcame this obstacle by adapting and improving a crosslinking affinity

bioRxiv preprint doi: https://doi.org/10.1101/159376; this version posted July 4, 2017. The copyright holder for this preprint (which was not certified by peer review) is the author/funder, who has granted bioRxiv a license to display the preprint in perpetuity. It is made available under aCC-BY 4.0 International license.

91 purification protocol (Weidner et al., 2014) to globally isolate P-body associated transcripts. We
92 demonstrate that P-bodies contain distinct mRNA species in response to specific stresses. The
93 sequestered transcripts underwent different fates depending on their function, for example:
94 mRNAs involved in overcoming stress were stabilized while others were degraded. Similarly,
95 mRNA decay kinetics differed depending on the mRNA examined. Our observations are
96 consistent with a dual role of P-bodies in mRNA degradation and storage. Under glucose
97 starvation, the RNA-binding protein Puf5p plays a central role as it regulates the decay of a set of
98 mRNAs and is also responsible for the localization and stability of another set. Moreover, the
99 stabilization of at least one mRNA in a Puf5-dependent manner may contribute to chronological
100 lifespan.

bioRxiv preprint doi: https://doi.org/10.1101/159376; this version posted July 4, 2017. The copyright holder for this preprint (which was not certified by peer review) is the author/funder, who has granted bioRxiv a license to display the preprint in perpetuity. It is made available under aCC-BY 4.0 International license.

101 **Results**

102

103 **A novel method to isolate RNAs sequestered into P-bodies**

104 To determine the mRNA species sequestered into P-bodies upon different stress conditions, we
105 combined and improved a method based on *in vivo* chemical crosslinking and affinity purification,
106 which we had previously used to identify regulators and protein components of P-bodies (Weidner
107 et al., 2014) with commonly used techniques to generate RNA libraries for subsequent RNA-Seq
108 (Hafner et al., 2010; Kishore et al., 2011) (Figure 1A). We refer to this method as chemical Cross-
109 Linking coupled to Affinity Purification (cCLAP). We have shown earlier that P-bodies in yeast are
110 in very close proximity to the endoplasmic reticulum (ER) and that they fractionate with ER
111 membranes (Kilchert et al., 2010; Weidner et al., 2014). To explore the mRNA content of P-bodies,
112 either Dcp2p or Scd6p, which are part of the 5' and the 3'UTR-associated complex of P-bodies,
113 respectively, were chromosomally tagged with a His_6-biotinylation sequence-His_6 tandem tag
114 (HBH) (Tagwerker et al., 2006; Weidner et al., 2014). P-bodies were either induced through
115 glucose starvation or through the addition of $CaCl_2$ or NaCl. We chose $CaCl_2$ as stressor because
116 secretory pathway mutants induce P-bodies through a Ca^{2+}/calmodulin-dependent pathway,
117 which is mimicked by the addition of Ca^{2+} to the medium (Kilchert et al., 2010). Notably, this
118 induction pathway is different from the one employed by the cell upon glucose starvation. NaCl
119 was selected as an alternative hyperosmotic stress to determine whether different hyperosmotic
120 stresses would elicit the same or different responses. We chose formaldehyde as cross-linking
121 agent because it can be directly applied to the culture medium and is easily and rapidly
122 quenchable allowing precise cross-linking conditions without introducing any unwanted stress like
123 through centrifugation or medium changes prior to the cross-link reaction. Yeast cells were
124 exposed to stress for 10 min, cross-linked and, after lysis, P-bodies were purified from the
125 membrane fraction through the HBH-tag present on either Dcp2p or Scd6p. We chose to stress
126 the cells for only 10 min in order to exclude any contribution of SG, which are not present at this

bioRxiv preprint doi: https://doi.org/10.1101/159376; this version posted July 4, 2017. The copyright holder for this preprint (which was not certified by peer review) is the author/funder, who has granted bioRxiv a license to display the preprint in perpetuity. It is made available under aCC-BY 4.0 International license.

Figure 1. RNA-Seq reveals stress-specific mRNA subsets enriched in P-bodies.
(A) RNA-Seq library preparation workflow. Cells expressing Dcp2-HBH or Scd6-HBH were stressed for 10 min, followed by cross-linking with formaldehyde. After cell lysis, centrifugation was performed to enrich membrane fractions. Cross-linked complexes were subsequently purified via streptavidin affinity purification. mRNAs were isolated and ligated with adapters. cDNA libraries were prepared by reverse transcription and sequenced using single-read RNA-Seq. (B) Venn diagram illustrating the intersections among mRNAs enriched in P-bodies (p<0.05) under glucose depletion and osmotic stress conditions with Na^{+} or Ca^{2+}, relative to the no stress condition as determined by RNA-Seq. (C) Read coverage plots (average over five biological replicates) of RNA-Seq data mapped to P-body enriched genes under specific stress conditions. (D) Enrichment analysis of P-body associated genes under different stress conditions against Gene Ontology's (GO) biological processes (BP). Significantly enriched pathways (q-value <0.05) from hypergeometric tests are presented in a clustered heatmap. Rows and columns correspond to stress conditions and pathways, respectively, and the negative logarithms of q-values are color-coded from blue (low) to red (high).

bioRxiv preprint doi: https://doi.org/10.1101/159376; this version posted July 4, 2017. The copyright holder for this preprint (which was not certified by peer review) is the author/funder, who has granted bioRxiv a license to display the preprint in perpetuity. It is made available under aCC-BY 4.0 International license.

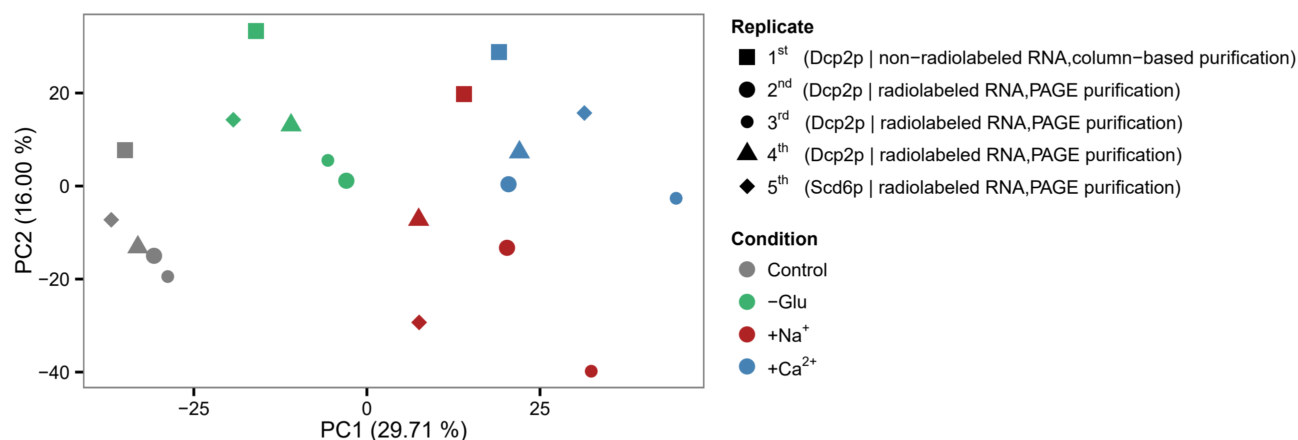

Figure 1- Figure Supplement 1. Reproducibility of datasets derived from RNA-Seq. Principal component analysis (PCA) plot based on the read count profile from aligned RNA-Seq data of five biological replicates for each condition. The two first principal components are plotted with the proportion of variance explained, indicated by each component next to the axes labels.

bioRxiv preprint doi: https://doi.org/10.1101/159376; this version posted July 4, 2017. The copyright holder for this preprint (which was not certified by peer review) is the author/funder, who has granted bioRxiv a license to display the preprint in perpetuity. It is made available under aCC-BY 4.0 International license.

127 time point (Kilchert et al., 2010). Libraries for RNA-Seq were prepared in two ways: either using
128 PAGE purification with radiolabeled mRNAs or using a column-based purification method (Table
129 S1).

130 Principal Component Analysis (PCA) performed on the read count profile for each
131 condition from the aligned RNA-Seq data of the five independent biological replicates generated
132 four clusters, corresponding perfectly to the three stress conditions plus the unstressed control
133 (Figure 1- Figure Supplement 1). Neither the tagged P-body component nor the purification
134 method used for RNA-Seq sample preparation perturbs the clustering pattern, indicating a high
135 degree of reproducibility of our method. Given that we used two types of hyperosmotic stress, it
136 is not surprising that the Ca^{2+} and Na^{+} datasets cluster more closely than the ones derived from
137 glucose starvation conditions. Yet, being able to detect differences between the two osmotic
138 shock conditions further exemplifies the robustness of our approach. Therefore, cCLAP is a valid
139 method to determine the RNA content of RNPs.

140 **The nature of P-body sequestered RNAs is stress-dependent**

141 In total, we identified 1544 mRNAs statistically significantly enriched in P-bodies under glucose
142 depletion and Na^{+} and Ca^{2+} stresses, relative to the unstressed condition (Figure 1B and Table
143 S2). While about 65% of the detected mRNAs were common between stresses, approximately
144 35% of the RNAs were specific to an individual stress (Figure 1B). Reads on stress-specific
145 targets were distributed over the entire length without any preferential accumulation or depletion
146 at the 5' or 3' UTRs as exemplified by the selected transcripts (Figure 1C).

147 If mRNA deposition in P-bodies was context-dependent, one would expect an enrichment
148 of mRNAs belonging to the same pathways/processes. To test this notion, we employed Gene
149 Ontology (GO) enrichment analysis (biological process) (Figure 1D). Consistent with the Venn
150 diagram (Figure 1B), a number of biological processes were shared by all three stress conditions,
151 yet many GO terms were specific to one particular stress, suggesting that mRNA sequestration
152 in P-bodies is, in general, context-dependent. For example, within the glucose specific set, we

bioRxiv preprint doi: https://doi.org/10.1101/159376; this version posted July 4, 2017. The copyright holder for this preprint (which was not certified by peer review) is the author/funder, who has granted bioRxiv a license to display the preprint in perpetuity. It is made available under aCC-BY 4.0 International license.

153 found a group of processes related to mitochondrial oxidative phosphorylation (herein referred to
154 as mitochondria-related mRNAs). This group is of particular interest, as mitochondria respiration
155 genes are generally up-regulated upon glucose starvation (Wu et al., 2004). Taken together, our
156 data suggest that a subset of mRNAs is sequestered in P-bodies in a stress-dependent manner.

157 **mRNAs localize to P-bodies in a context-dependent manner**

158 Thus far, we have shown that mRNAs can be cross-linked to P-body components in a stress-
159 dependent manner. To demonstrate that these mRNAs indeed localize to P-bodies, we employed
160 fluorescence *in situ* hybridization coupled to immunofluorescence (FISH-IF; Figure 2A). We used
161 Dcp2p as P-body marker for immunofluorescence. Since P-bodies exhibit a compact, dense
162 structure (Souquere et al., 2009), the generally employed long probes (up to 1,000 nt) are not
163 suitable for detection of mRNA in P-bodies. However, using multiple 50-100 nt FISH probes (4-8
164 per transcript) allowed us to detect specific mRNAs in P-bodies, as the no probe control only
165 exhibited background staining (Figure 2, Figure 2- Figure Supplement 1A). Regardless, we may
166 not be able to detect all mRNA molecules and are likely underestimating the extent of localization
167 of mRNAs within P-bodies. Moreover, transcripts in yeast are often present in less than 10 copies
168 per cell (Zenklusen et al., 2008), which may hinder detection by this method. Finally, most mRNAs
169 are degraded in P-bodies (Sheth and Parker, 2003), therefore any given mRNA may be detected
170 in P-bodies at any given time. Taken theses constraints into consideration, we set the threshold
171 at ≥ 1.5 fold enrichment over control mRNAs to determine P-body association.

172 We selected a set of mRNAs from each stress condition and determined their subcellular
173 localization. Upon glucose depletion, seven mRNAs including both non-mitochondria-related
174 (*BSC1*, *TPI1*, *RLM1*) and mitochondria-related (*ATP11*, *ILM1*, *MRPL38*, *AIM2*) groups, based on
175 the GO pathways, showed significant co-localization with P-bodies (Figure 2B, 2C) relative to
176 background (Figure 2- Figure Supplement 1B, C). To validate that the mRNA localization to P-
177 bodies is stress-specific, we repeated the FISH-IF under osmotic stresses for three mRNAs
178 (Figure 2D). None of them was significantly enriched in P-bodies under these stress conditions

bioRxiv preprint doi: https://doi.org/10.1101/159376; this version posted July 4, 2017. The copyright holder for this preprint (which was not certified by peer review) is the author/funder, who has granted bioRxiv a license to display the preprint in perpetuity. It is made available under aCC-BY 4.0 International license.

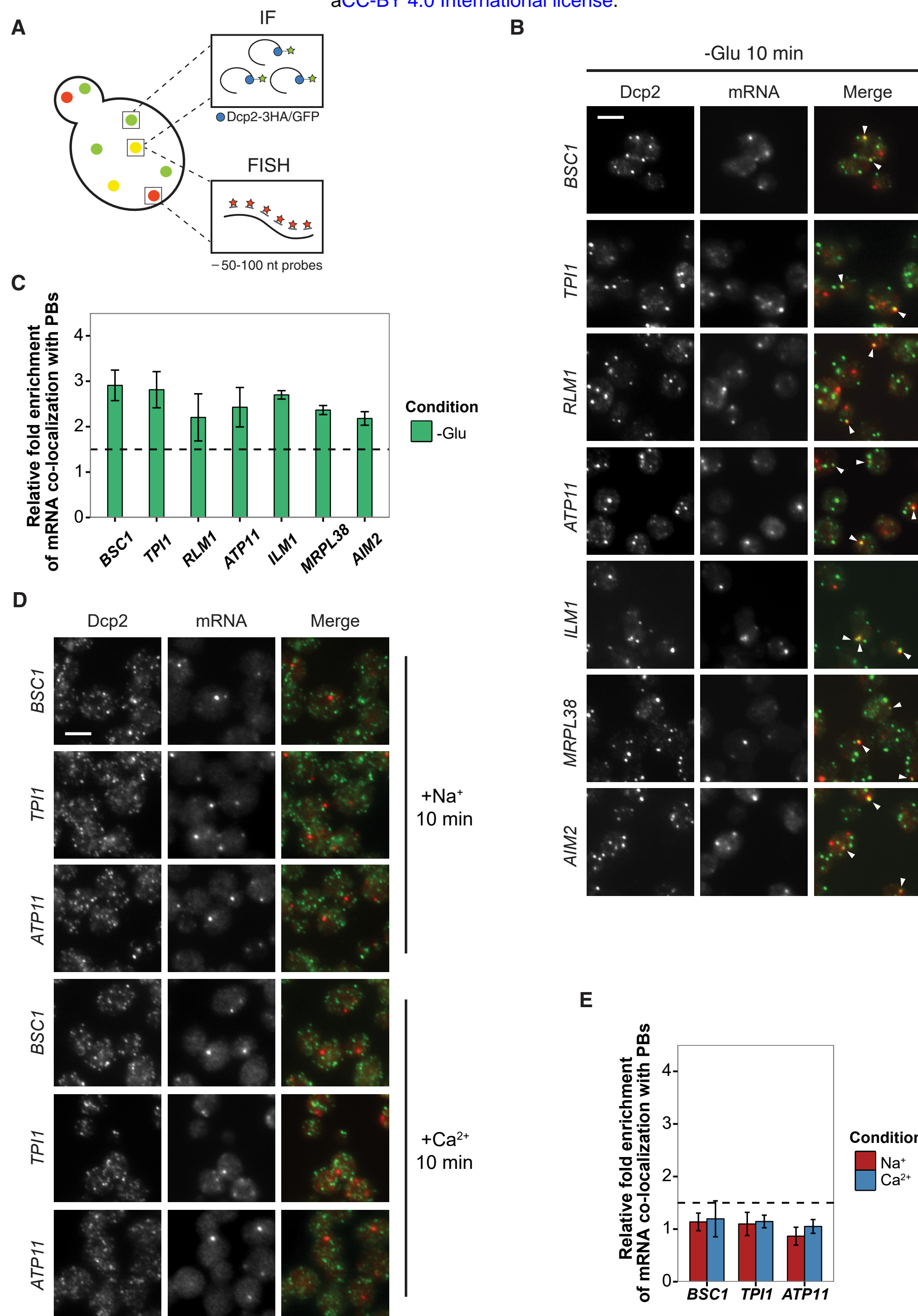

Figure 2. Validation of glucose-specific candidates by combined fluorescence in situ hybridization and immuno-fluorescence (FISH IF).

(A) Schematic representation of combined FISH-IF technique. Immunofluorescence staining was performed against P-body marker Dcp2 chromosomally tagged with 3HA or GFP. To detect mRNAs accumulating in P-bodies, multiple short probes (50-100 nt) against the open reading frame (ORF) of each gene were used for FISH. (B) Fluorescence images of P-bodies and glucose-starvation-specific candidate mRNAs after glucose depletion. Cells expressing Dcp2-3HA were first grown in YPD media to mid-log phase and shifted to YP media lacking glucose for 10 min. Scale bar, 5 µm. Error bars, Mean ± SEM. (C) Bar plot depicting the quantification of co-localization between candidate mRNAs and P-bodies. The percentage of co-localization was quantified as described in Materials and Methods. The relative fold enrichment was subsequently calculated by normalizing the percentage of candidate mRNAs against the percentage of control mRNAs (Figure 2- Figure Supplement 1C). The dashed line represents an arbitrarily fixed threshold of 1.5 for determining significant P-body association. (D) Fluorescence images of P-bodies and glucose-specific candidate mRNAs under mild osmotic stress with Na^{+} or Ca^{2+}. Cells expressing Dcp2-3HA were first grown in YPD media to mid-log phase and shifted to YPD media containing 0.5 M NaCl or 0.2 M $CaCl_2$ for 10 min. Scale bars, 5 µm. Error bars, Mean ± SEM. (E) Same as (C) except stress conditions. Scale bar, 5 µm. Error bars, Mean ± SEM.

bioRxiv preprint doi: https://doi.org/10.1101/159376; this version posted July 4, 2017. The copyright holder for this preprint (which was not certified by peer review) is the author/funder, who has granted bioRxiv a license to display the preprint in perpetuity. It is made available under aCC-BY 4.0 International license.

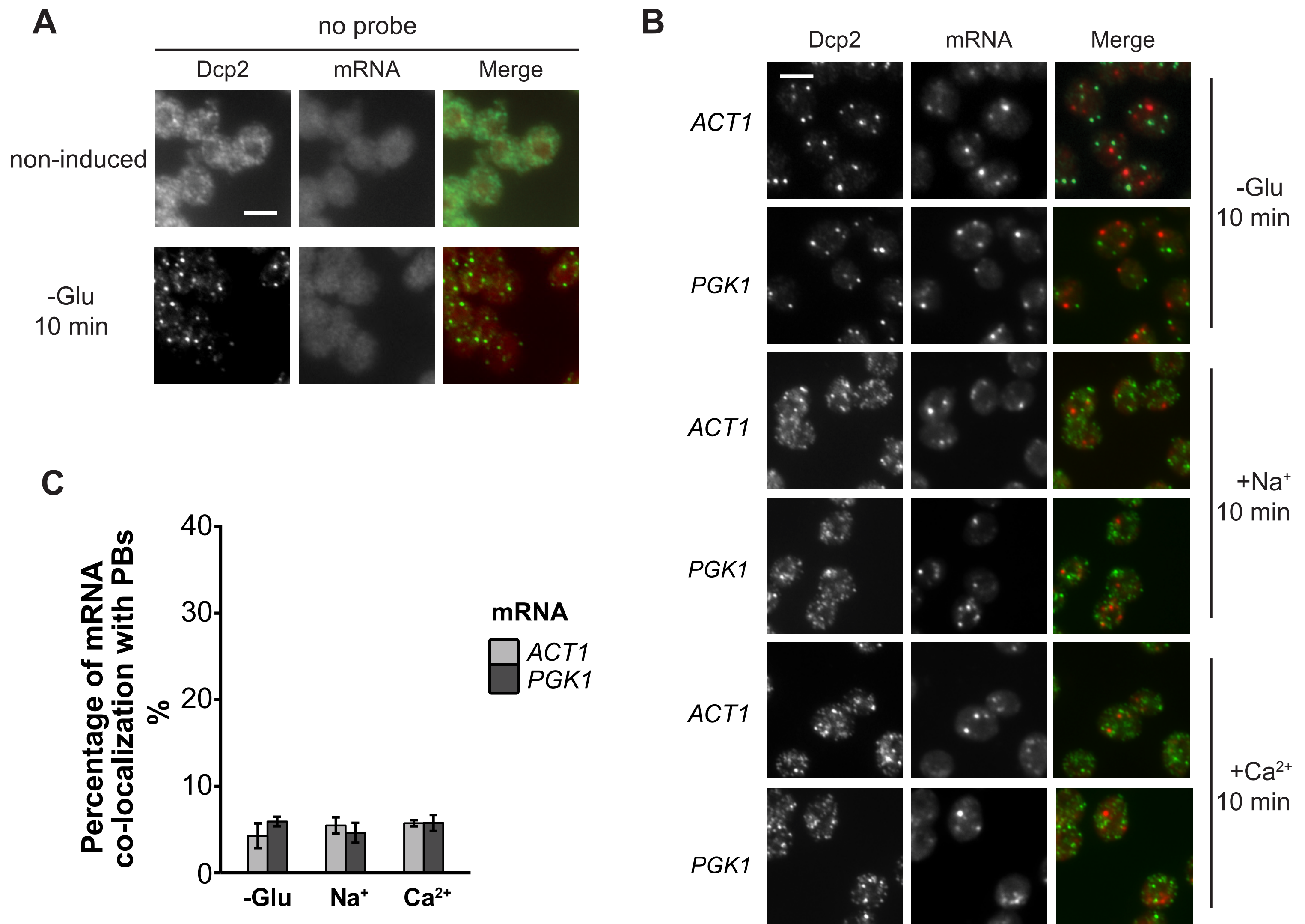

Figure 2- Figure Supplement 1. Evaluation of non-candidate mRNAs by FISH-IF.
(A) FISH-IF controls. Combined FISH-IF was performed without probes with cells expressing Dcp2-3HA under non-induced condition. Scale bar, 5 μm. (B) Fluorescence images of P-bodies and two non-candidate mRNAs, *ACT1* and *PGK1*. Cells expressing Dcp2-3HA were treated with indicated stresses. Scale bar, 5 μm. (C) Bar plot depicting the percentage of co-localization between non-candidate mRNAs and P-bodies. The average of the percentages of *ACT1* and *PGK1* under each condition served as a control level in calculating the fold enrichment in Figure 2C, 2E, 4B, 5C and 4S1D. Error bars, Mean ± SEM. Scale bar, 5 μm.

bioRxiv preprint doi: https://doi.org/10.1101/159376; this version posted July 4, 2017. The copyright holder for this preprint (which was not certified by peer review) is the author/funder, who has granted bioRxiv a license to display the preprint in perpetuity. It is made available under aCC-BY 4.0 International license.

179 (Figure 2E). Similarly, we found mRNAs that were specifically enriched in P-bodies under a
180 unique osmotic condition but not under the other stresses (data not shown). We conclude that at
181 least a subset of mRNAs must be selected for -or spared from- transport to P-bodies in a context-
182 dependent manner.

183 **mRNAs experience divergent fates inside P-bodies**

184 It has been proposed that mRNAs are not only decayed in P-bodies, but may be stored there and
185 re-enter translation after stress subsides (Brengues et al., 2005). We found mRNAs that were
186 potentially excellent candidates for being stored in P-bodies. The mitochondria-related genes
187 were transcriptionally up-regulated following glucose starvation (Figure 3- Figure Supplement 1A),
188 while at the same time transcripts were sequestered in P-bodies. To investigate the fate of P-
189 body associated mRNAs further, we employed the 4-TU non-invasive pulse-chase RNA labeling
190 technique followed by qRT-PCR. With this technique, we can specifically label RNA before stress
191 application and determine its decay rate (Munchel et al., 2011) (Figure 3A). To differentiate P-
192 body specific degradation from the exosome decay pathway, we analyzed the mRNA half-life in
193 the presence and absence of the P-body 5'-3' exonuclease Xrn1p (Figure 3B). *ACT1* was used
194 as endogenous reference gene due to its high stability during glucose starvation (Figure 3- Figure
195 Supplement 1B). No significant reduction in mRNA levels was observed for Group II mRNAs
196 (*ATP11*, *ILM1*, *MRPL38* and *AIM2*) for up to one hour of glucose withdrawal, suggesting that
197 those transcripts were stabilized inside P-bodies (Figure 3B, Group II). Consistently, after a rapid
198 initial increase, the total transcript levels remained constant over the time course (Figure 3- Figure
199 Supplement 1A, Group II). Conversely, the transcripts within group I (*BSC1*, *TPI1*, and *RLM1*)
200 underwent Xrn1p-dependent decay (Figure 3B, Group I). Intriguingly, the onset and the kinetic of
201 the decay varied from mRNA to mRNA, indicating that individual intrinsic properties of the mRNAs
202 may determine their half-lives within P-bodies. Likewise, the total mRNA levels were modulated
203 in a similar way (Figure 3- Figure Supplement 1A, Group I), hinting towards coordination between
204 P-body specific decay and transcription. Our data provide strong evidence that the decay kinetics

bioRxiv preprint doi: https://doi.org/10.1101/159376; this version posted July 4, 2017. The copyright holder for this preprint (which was not certified by peer review) is the author/funder, who has granted bioRxiv a license to display the preprint in perpetuity. It is made available under aCC-BY 4.0 International license.

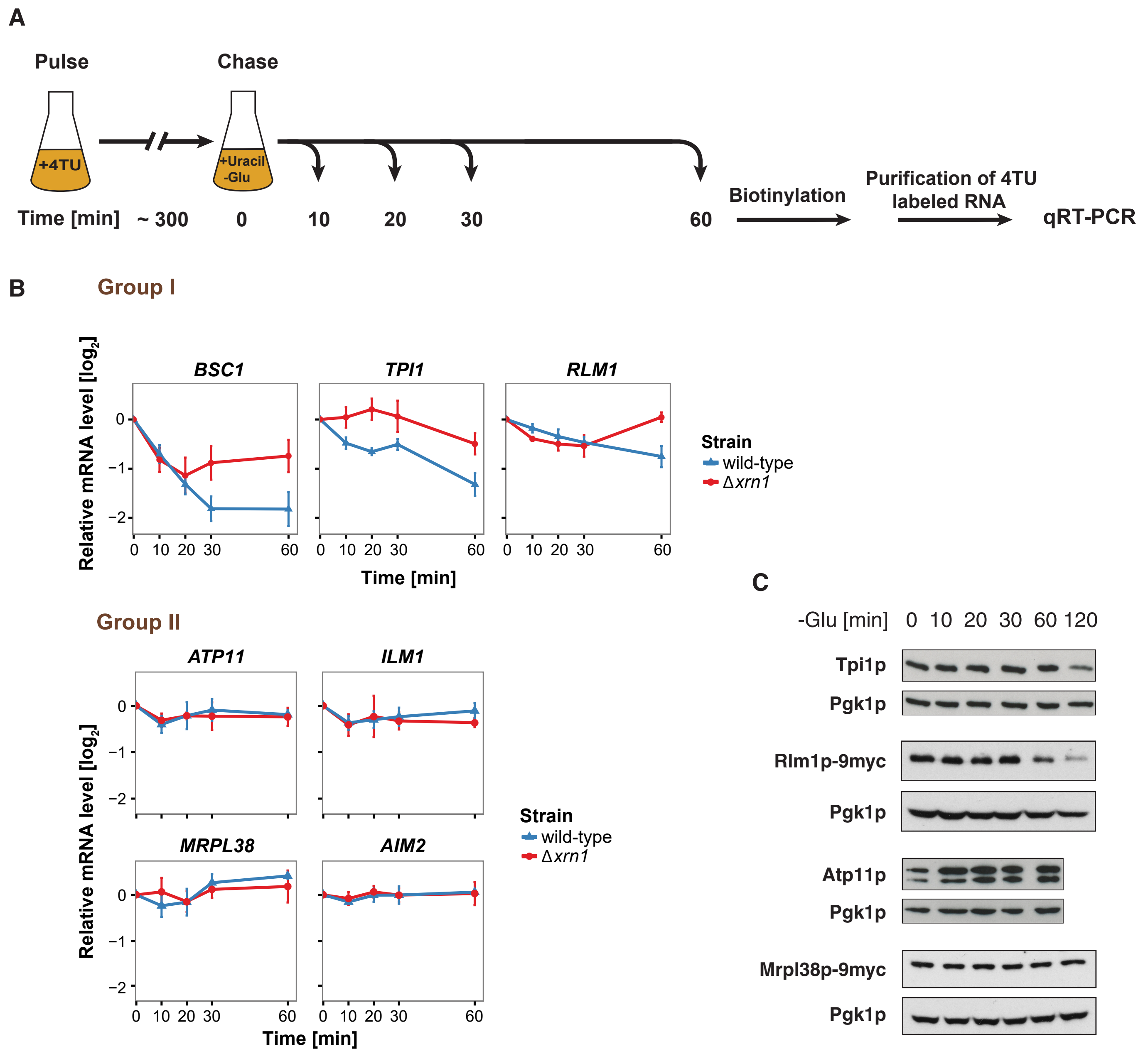

Figure 3. The stability of P-body enriched mRNAs varies and can be categorized according to their GO terms. (A) Schematic illustration of pulse-chase protocol. Cells were grown in the presence of 0.2 mM 4TU and shifted into media lacking glucose but containing 20 mM uracil. Cells were harvested at indicated time points after the shift. Total RNA was extracted and biotinylated. 4TU labeled RNA was purified and subsequently analyzed by qRT-PCR. (B) The stability of 4TU labeled candidate mRNAs was determined by qRT-PCR in wild type and Δ*xrn1* strains at indicated time points following a shift to glucose-depleted media. Transcription levels were normalized using *ACT1* gene as an endogenous reference. Group I: non-mitochondria-related candidates. Group II: mitochondria-related candidates. Error bars, Mean ± SEM. (C) Western blot analysis of Tpi1p, Rlm1p-9myc, Atp11p and Mprl38p-9myc at indicated time points after glucose deprivation. The 9myc tag was inserted at the end of the coding sequence without affecting the 3'UTR. Pgk1p was used as a loading control. Anti-Tpi1p, anti-Atp11p, anti-myc and anti-Pgk1p were used for detection. Results are representative of 3-4 independent experiments per target protein.

bioRxiv preprint doi: https://doi.org/10.1101/159376; this version posted July 4, 2017. The copyright holder for this preprint (which was not certified by peer review) is the author/funder, who has granted bioRxiv a license to display the preprint in perpetuity. It is made available under aCC-BY 4.0 International license.

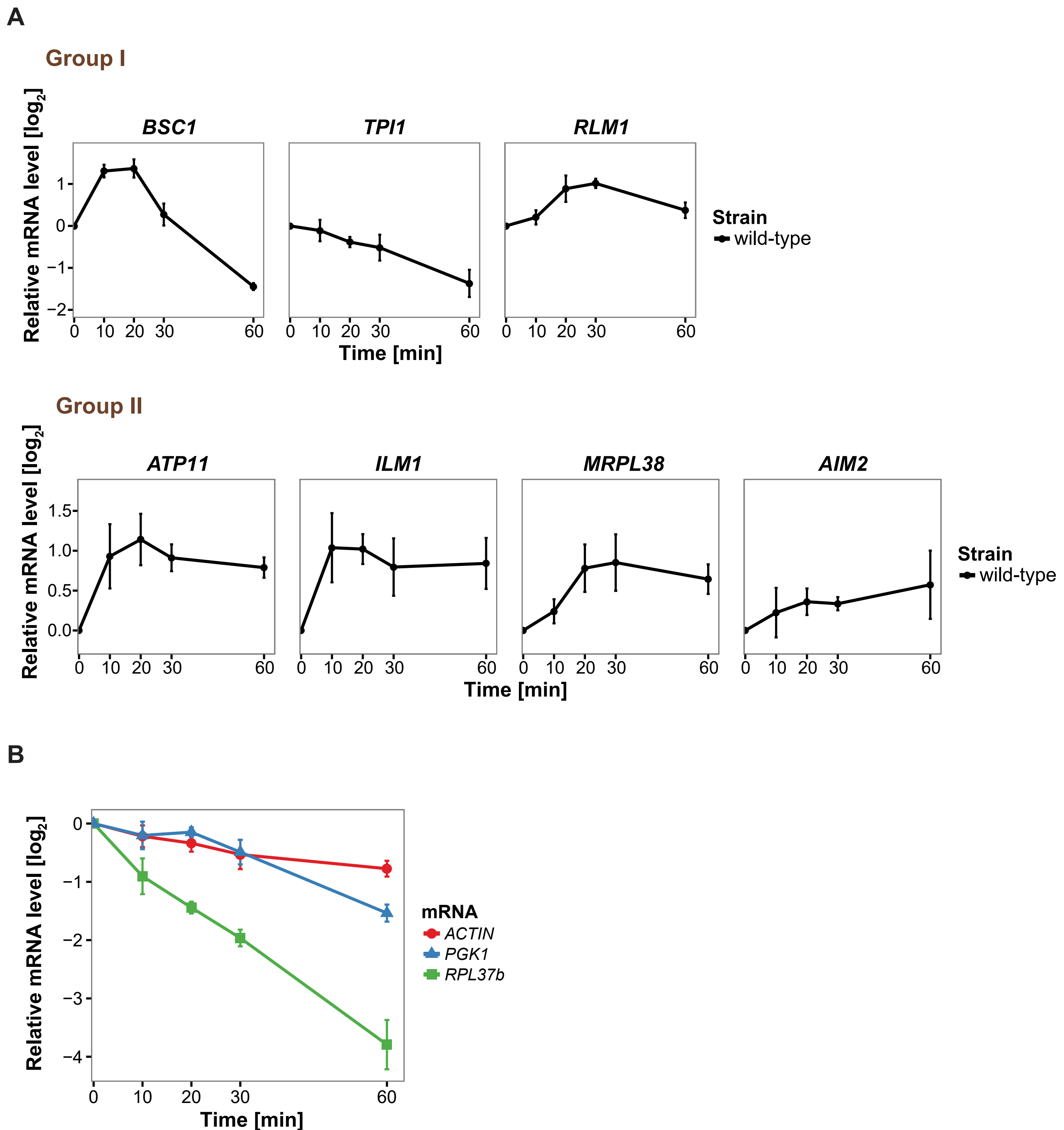

Figure 3- Figure Supplement 1. Changes in total candidate mRNA levels corresponding to Xrn1-dependent degradation.

(A) Evaluation of qRT-PCR reference genes stability after glucose depletion. The total mRNA levels of three commonly used reference genes were measured by qRT-PCR and normalized to spike-in RNA control as described in Materials and Methods. Error bars, Mean ± SEM. (B) Fold changes of total candidate mRNA levels after glucose depletion were determined by qRT-PCR using *ACT1* as reference. Group I: non-mitochondria-related candidates. Group II: mitochondria-related candidates. Error bars, Mean ± SEM.

bioRxiv preprint doi: https://doi.org/10.1101/159376; this version posted July 4, 2017. The copyright holder for this preprint (which was not certified by peer review) is the author/funder, who has granted bioRxiv a license to display the preprint in perpetuity. It is made available under aCC-BY 4.0 International license.

205 and stability of mRNAs within P-bodies depend on individual properties, and that mRNAs acting
206 in the same process might be co-regulated.

207 Next, we asked whether the fate of an mRNA has an impact on its translation product.
208 Therefore, we assessed the protein level of Tpi1p and Rlm1 (Group I) as well as Atp11p and
209 Mrpl38p (Group II) upon glucose depletion over time (Figure 3C). Consistent with the changes in
210 mRNA levels, Group I protein levels dropped, while the Group II protein levels remained stable or
211 increased over the glucose starvation time course. Our results reveal distinct and separable roles
212 of P-bodies in regulating mRNA stabilities. On one hand, P-bodies contain transcripts undergoing
213 decay in an individually regulated time-dependent manner. On the other hand, another group of
214 mRNAs, whose protein product contributes to stress response, are protected by P-bodies.

215 **Puf5p contributes to both recruitment and decay of P-body mRNAs**

216 Next, we aimed to record the transport of mRNAs into P-bodies by live-cell imaging using the well-
217 established MS2 and U1A systems (Chung and Takizawa, 2011; Zenklusen et al., 2007). Tagging
218 transcripts with U1A stem loops massively induced P-body formation under non-stress conditions
219 (data not shown). Similarly, appending candidate transcripts with MS2 loops increased the co-
220 localization of mRNA and P-body components to almost 100% (Figure 4- Figure Supplement 1),
221 which is in marked contrast to the FISH data. This high degree of co-localization can be explained
222 by the recent finding that highly repetitive stem-loops can lead to non-degradable 3' mRNA
223 fragments causing mislocalization of tagged mRNAs (Garcia and Parker, 2015). Considering the
224 strong discrepancy between the FISH and MS2 localization data in terms of extent of P-body
225 localization, and the recently published potential aberrant localization of MS2-tagged mRNAs, we
226 decided to use the more conservative and less errror-prone FISH-IF method to identify factors
227 required for the localization and/or fate of mRNAs in P-bodies. We explored several known protein
228 factors, which may contribute to this process with a candidate approach using *BSC1* (Group I)
229 and *ATP11* (Group II) probes (Figure 4- Figure Supplement 2A). We deleted known P-body

bioRxiv preprint doi: https://doi.org/10.1101/159376; this version posted July 4, 2017. The copyright holder for this preprint (which was not certified by peer review) is the author/funder, who has granted bioRxiv a license to display the preprint in perpetuity. It is made available under aCC-BY 4.0 International license.

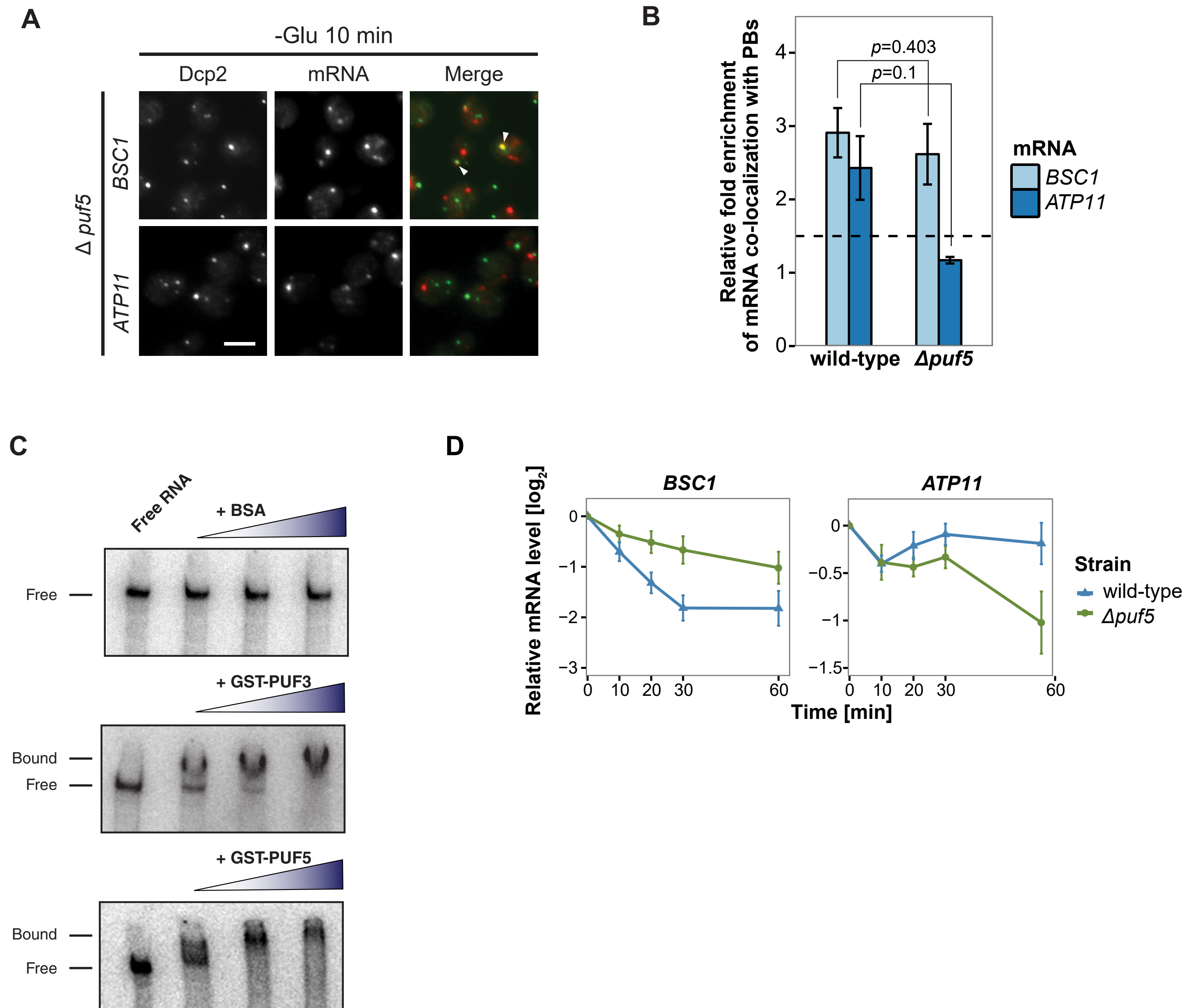

Figure 4. Puf5p is required for both mRNA recruitment and regulation of mRNA decay in P-bodies.
(A) Fluorescence images of P-bodies and *BSC1* (Group I) or *ATP11* (Group II) mRNAs following glucose depletion on Δ*puf5* cells expressing Dcp2-GFP. Scale bar, 5 μm. (B) Bar plot showing the relative fold enrichment of co-localization between *BSC1*, *ATP11* and P-bodies in Δ*puf5* strain 10 min after switched to glucose-free media. Wild type is plotted as in Figure 2C. The dashed line represents a fixed threshold of 1.5 for determining significant enrichment. Error bars, Mean ± SEM. A one-tailed, non-paired Student's *t*-test was used to determine *p* values. (C) EMSA assays using *ATP11* 3'UTR RNA (1-500 nt after STOP codon) oligonucleotide in the absence or presence of bovine serum albumin (1.25, 2.5, 5 μ M), GST-PUF3 (10, 50, 100 nM) and GST-PUF5 (1.25, 2.5, 5 μM). Unbound radiolabelled RNA (Free) shifts to a high molecular weight complex when bound to GST-PUF3 or GST-PUF5 (Bound), Results are representative of 3-4 independent experiments per protein. (D) The stability of 4-TU labeled *BSC1* and *ATP11* mRNAs was measured by qRT-PCR in Δ*puf5* strain at indicated time points following glucose depletion. Wild type is plotted as in Figure 3B. Error bars, Mean ± SEM.

bioRxiv preprint doi: https://doi.org/10.1101/159376; this version posted July 4, 2017. The copyright holder for this preprint (which was not certified by peer review) is the author/funder, who has granted bioRxiv a license to display the preprint in perpetuity. It is made available under aCC-BY 4.0 International license.

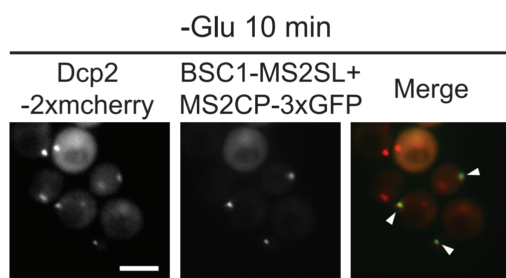

Figure 4- Figure Supplement 1. Live-cell detection of P-bodies (Dcp2-2xmcherry) and *BSC1* mRNA molecules using the MS2 system. Scale bar, 5 μm. Results are representative of 3 independent experiments.

bioRxiv preprint doi: https://doi.org/10.1101/159376; this version posted July 4, 2017. The copyright holder for this preprint (which was not certified by peer review) is the author/funder, who has granted bioRxiv a license to display the preprint in perpetuity. It is made available under aCC-BY 4.0 International license.

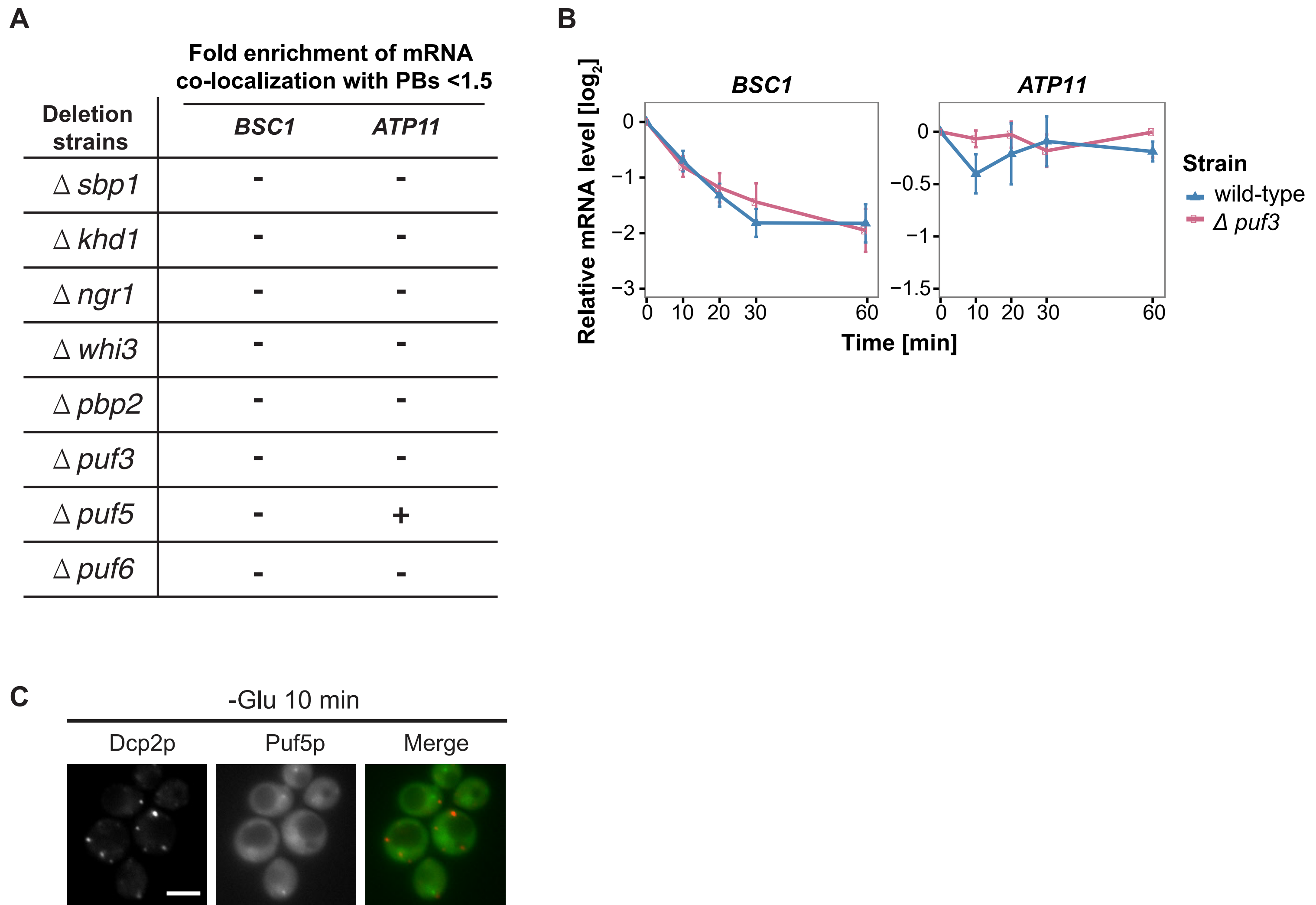

Figure 4- Figure Supplement 2. A screen for RNA-binding proteins required for mRNA recruitment to P-bodies. (A) A screen to identify RNA-binding proteins affecting mRNA recruitment to P-bodies by FISH-IF. *BSC1* and *ATP11* were selected for screening performed with the deletion strains as listed. A fold enrichment value above 1.5 was classified as not required (-), below as required (+). Two independent experiments were performed per mRNA per strain. (B) The stability of 4-TU labeled *BSC1* and *ATP11* mRNAs was measured by qRT-PCR in Δ*puf3* strain at indicated time points following glucose depletion. Wild type is plotted as in Figure 3B. Error bars, Mean ± SEM. (C) Live-cell detection of P-bodies (Dcp2-2xmcherry) and Puf5p (GFP) following glucose withdrawal, Scale bar, 5 µm. Results are representative of 3 independent experiments.

bioRxiv preprint doi: https://doi.org/10.1101/159376; this version posted July 4, 2017. The copyright holder for this preprint (which was not certified by peer review) is the author/funder, who has granted bioRxiv a license to display the preprint in perpetuity. It is made available under aCC-BY 4.0 International license.

230 components or factors associating with P-bodies upon glucose deprivation (Sbp1p, Khd1p, Ngr1p
231 and Whi3p) (Cai and Futcher, 2013; Mitchell et al., 2013) and candidates known to promote
232 mRNA decay or repress mRNA translation, including poly(A)-binding protein II (Pbp2p), two PUF
233 family proteins (Puf3p and Puf5p) and one non-canonical PUF protein (Puf6p) (Chritton and
234 Wickens, 2010; Wickens et al., 2002). Remarkably, the loss of Puf5p efficiently inhibited the
235 recruitment of *ATP11* to P-bodies as the co-localization dropped to background levels (Figure 4A,
236 4B). In contrast, *BSC1* localization was unaffected (Figure 4A, 4B). The observed lack of *ATP11*
237 P-body localization in *Δpuf5* cells was specific, since none of the other deletion strains showed a
238 targeting defect (Figure 4- Figure Supplement 2A). To investigate the consequence of the inability
239 of *ATP11* to be protected in P-bodies in Δ*puf5*, we determined the *ATP11* mRNA levels. Indeed,
240 *ATP11* mRNA levels declined, when no longer associated with P-bodies (Figure 4C). These data
241 confirm that *ATP11* mRNA is protected in P-bodies from decay.

242 Conversely, the localization of *BSC1* mRNA to P-bodies was not altered in cells lacking
243 Puf5p and the mRNA seemed to be stabilized to a certain degree, consistent with Puf5p's role in
244 mRNA decay (Goldstrohm et al., 2006). Recent data suggest that Puf5p binds to both *BSC1* and
245 *TPI1* mRNA, but not to any of the candidates of Group II (Wilinski et al., 2015). In contrast, *ATP11*
246 has been reported to be a target of Puf3p (Gerber et al., 2004). However, in Δ*puf3* neither the
247 localization to P-bodies nor *ATP11* stability was affected, suggesting Puf3p is presumably not
248 essential for P-body related *ATP11* regulation upon glucose deprevation (Figure 4- Figure
249 Supplement 2B). Even though, others and we were unable to detect Puf5p in P-bodies (Figure
250 4- Figure Supplement 2C) (Goldstrohm et al., 2006), it is still possible that Puf5p interacts with
251 *ATG11*. To address this possibility, we performed electro mobility shift assays (EMSAs) with 500
252 bp of the *ATP11* 3'UTR and Puf3p and Puf5p. (Figure 4D). Both Puf3p and Puf5p, but not BSA
253 bound the *ATP11* 3'UTR, albeit the Puf5p binding affinity being much weaker. Neither *ATP11* nor
254 any of the other Group II mRNAs tested, contains a recognizable Puf5-binding sequence,

bioRxiv preprint doi: https://doi.org/10.1101/159376; this version posted July 4, 2017. The copyright holder for this preprint (which was not certified by peer review) is the author/funder, who has granted bioRxiv a license to display the preprint in perpetuity. It is made available under aCC-BY 4.0 International license.

255 indicating the presence of a non-canonical binding site. Our data suggest that Puf5p directly
256 controls *BSC1* and *ATP11* mRNA stability and *ATP11* mRNA localization.

257 **The 3'UTR is necessary but not sufficient for mRNA targeting to P-bodies**

258 Considering that the 3'UTR of mRNAs contains most regulatory elements, which often have an
259 important role in determining mRNA localization (Andreassi and Riccio, 2009; Vuppalanchi et al.,
260 2010), we next investigated whether 3'UTRs play a role in mRNA targeting to P-bodies. We
261 replaced the endogenous 3'UTR of *BSC1* and *ATP11* with the 3'UTR of *K. lactis TRP1* (*klTRP1*)
262 and examined the localization of the chimera by FISH-IF after glucose starvation (Figure 5A).
263 Replacing the 3'UTR abolished recruitment of both mRNAs to P-bodies (Figure 5B, 5C),
264 suggesting that even though the localization signal must be different between *ATP11* and *BSC1*,
265 the necessary sequences are present in the 3'UTR. Consistent with the mislocalization, *BSC1*
266 and *ATP11* transcripts were stabilized and degraded, respectively (Figure 5D). The destabilization
267 of the *ATP11* mRNA is also reflected in the reduction of Atp11p protein levels under the same
268 conditions. Thus, the 3'UTR is essential for the fate and P-body localization under glucose
269 starvation for both transcripts.

270 Since the 3'UTR was essential for both mRNAs, we investigated whether common primary
271 sequence motifs between all mRNAs, which were specifically enriched in P-bodies under a unique
272 stress, exist using the MEME Suite (Bailey et al., 2009). Probably not so unexpected, we did not
273 find any significant primary sequence conservations or enrichment, of any particular motif. Next,
274 we clustered stress-dependent P-body mRNAs based on secondary structures within the 3'UTR
275 using NoFold (Middleton and Kim, 2014). In comparison to non-candidate mRNAs, each stress-
276 specific candidate set contained 10-20 clusters of transcripts that were differentially enriched in
277 certain structure motifs (Table S2). Interestingly, enriched motifs exhibited strong similarities (Z-
278 score > 3) to known miRNA motifs from RFAM, in line with the observation that at least in
279 mammalian cells and *Drosophila*, P-bodies were shown to contain miRNA silencing complex
280 components (Liu et al., 2005; Sen and Blau, 2005). One possible explanation is that general stem-

bioRxiv preprint doi: https://doi.org/10.1101/159376; this version posted July 4, 2017. The copyright holder for this preprint (which was not certified by peer review) is the author/funder, who has granted bioRxiv a license to display the preprint in perpetuity. It is made available under aCC-BY 4.0 International license.

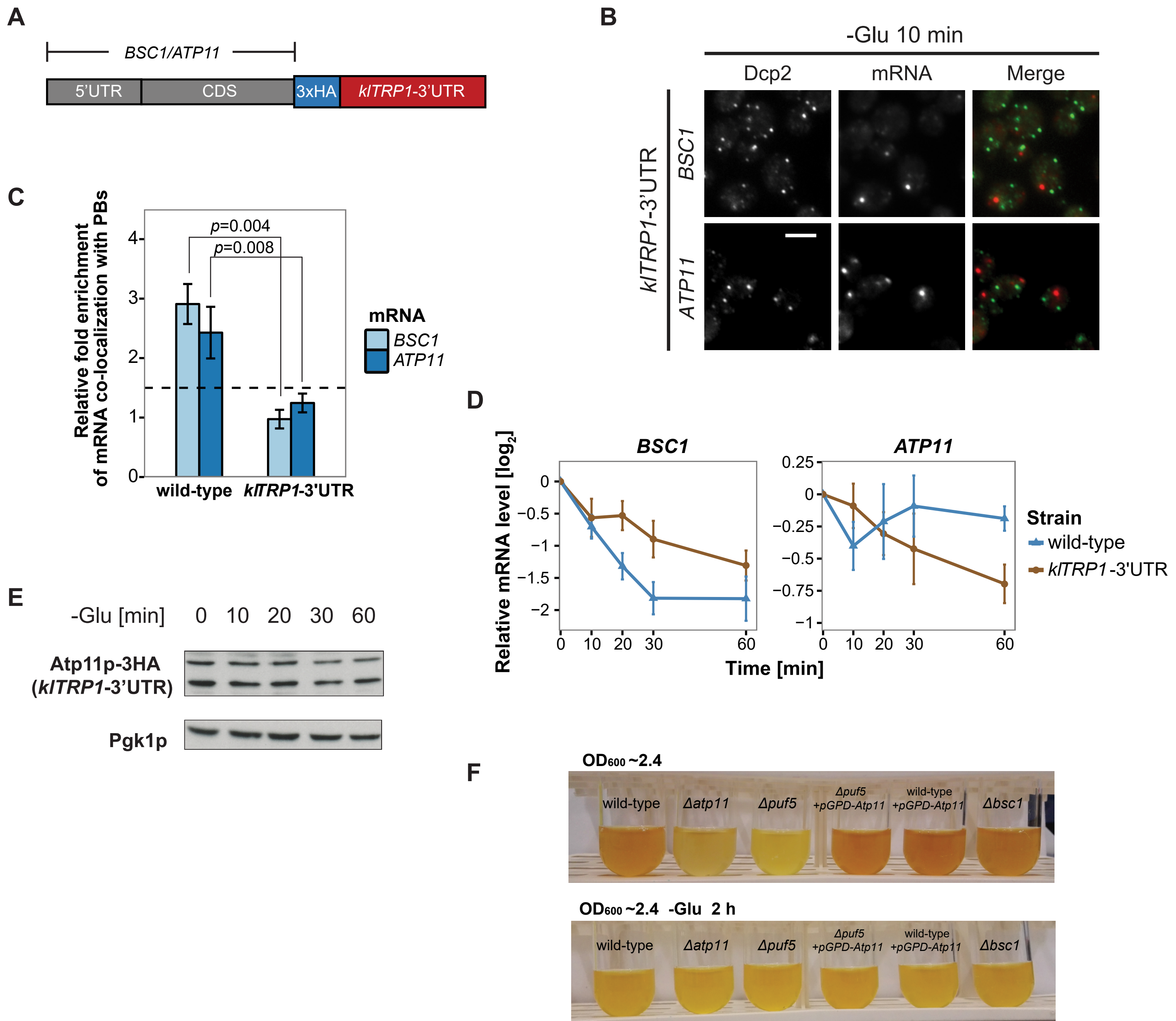

Figure 5. 3'UTR is necessary for mRNA localization to P-bodies.
(A) A schematic representation of C terminal tagging with 3x HA. The endogenous 3'UTR was simultaneously replaced by the 3'UTR of *klTRP1*. (B) Fluorescence images of P-bodies and *BSC1*, *ATP11* mRNAs following glucose depletion on corresponding 3'UTR replaced strains. Scale bar, 5 µm. (C) Bar plot depicting the relative fold enrichment of co-localization between *BSC1*, *ATP11* and P-bodies in corresponding 3'UTR replaced strains 10 min after glucose starvation. Wild type is plotted as in Figure 2C. The dashed line represents a fixed threshold of 1.5 for determining significant enrichment. Error bars, Mean ± SEM. A one-tailed, non-paired Student's *t*-test was used to determine *p* values. (D) The stability of 4TU labeled *BSC1* and *ATP11* mRNAs was determined by qRT-PCR in corresponding 3'UTR replaced strains at indicated time points following glucose depletion. Wild type is plotted as in Figure 3B. Error bars, Mean ± SEM. (E) Western blot analysis of Atp11-HA (*klTRP1* 3'UTR) at indicated time points after glucose deprivation. Pgk1 was used as a loading control. Anti-HA and anti-Pgk1p were used for detection. Results are representative of 3 independent experiments. (F) Assessment of intracellular glycogen content in wild type, *ATP11*, *PUF5* deletion strains in the absence or presence of *ATP11* overexpression plasmid and *BSC1* deletion strain by iodine staining. Yeast cultures were grown to stationary phase (OD_{600} ~2.4) in medium containing 2% dextrose (upper panel). Then cells were shifted to medium without dextrose for 1 h (lower panel). Results are representative of 4 independent experiments.

bioRxiv preprint doi: https://doi.org/10.1101/159376; this version posted July 4, 2017. The copyright holder for this preprint (which was not certified by peer review) is the author/funder, who has granted bioRxiv a license to display the preprint in perpetuity. It is made available under aCC-BY 4.0 International license.

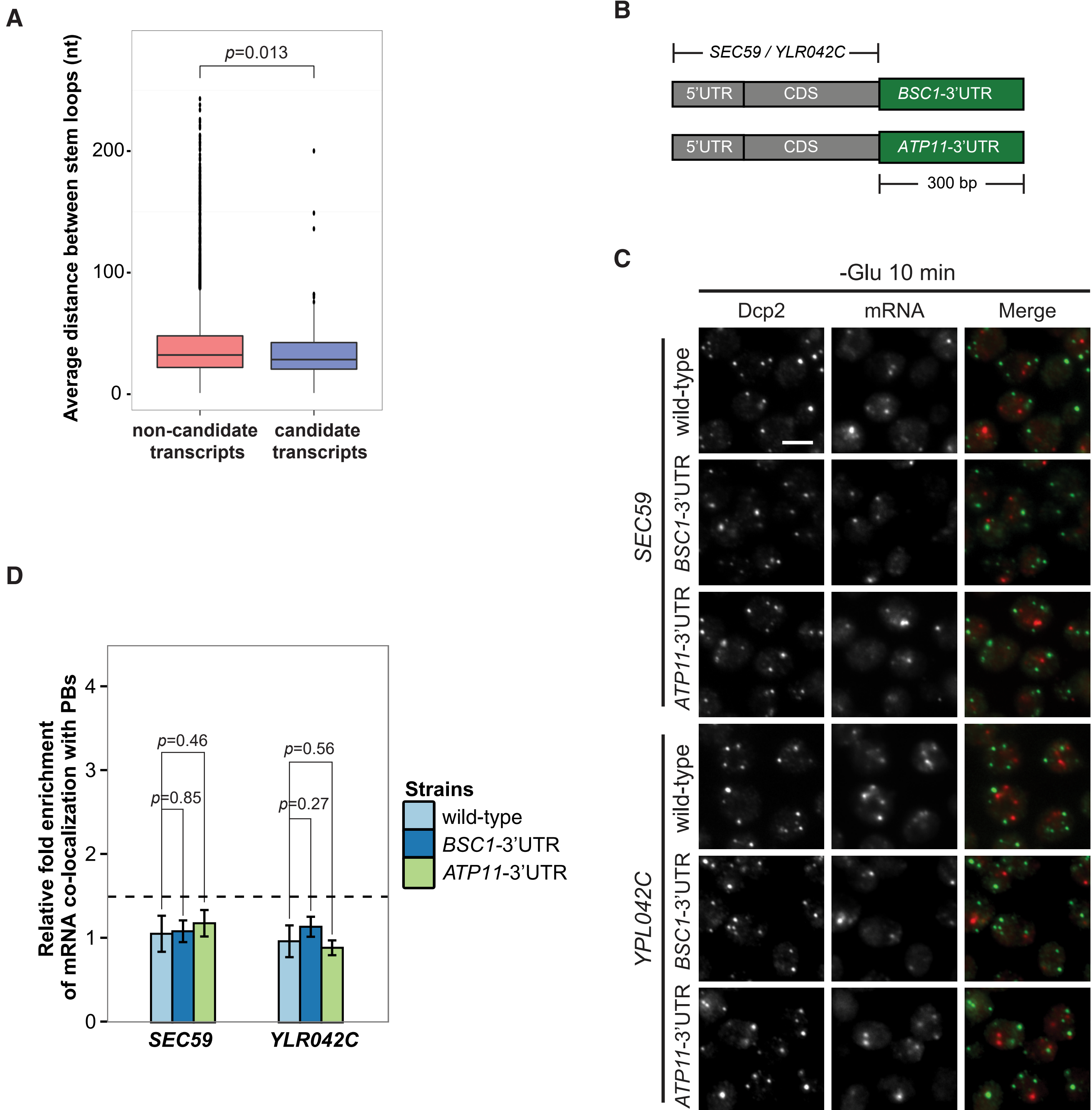

Figure 5- Figure Supplement 1. 3'UTR is insufficient for mRNA localization to P-bodies.
(A) Box plot of average distances between stem loops among the 3'UTRs of candidate transcripts versus non-candidate transcripts. A non-parametric, one-sided Wilcoxon rank-sum test was used to determine *p* values. (B) A schematic representation of 3'UTR transplantation chimeras. The endogenous 3'UTRs (300 bp downstream from stop codon) of *SEC59* and *YLR042C* (300 bp downstream from stop codon) were replaced by the 3'UTRs of *BSC1* and *ATP11*, respectively. (C) Fluorescence images of P-bodies and *SEC59* and *YLR042C* mRNAs following glucose depletion. Scale bar, 5 μm. (D) Bar plot showing the relative fold enrichment of co-localization between *SEC59*, *YLR042C* and P-bodies in indicated chimeric strains 10 min after glucose withdrawal. Wild type is plotted as in Figure 2C. The dashed line represents a fixed threshold of 1.5 for determining significant enrichment. Error bars, Mean ± SEM. A one-tailed, non-paired Student's *t*-test was used to determine *p* values.

bioRxiv preprint doi: https://doi.org/10.1101/159376; this version posted July 4, 2017. The copyright holder for this preprint (which was not certified by peer review) is the author/funder, who has granted bioRxiv a license to display the preprint in perpetuity. It is made available under aCC-BY 4.0 International license.

281 loop structures may favor P-body localization under stress. To test this hypothesis, we determined
282 the predicted number of stem loops in the 3'UTR of mRNAs enriched specifically under stress
283 versus inert mRNAs and calculated the distance between stem loops. We observed a decrease
284 in the distance between stem loops, suggesting clustering of the loops (Figure 5- Figure
285 Supplement 1A). To determine whether clusters of stem loops would be sufficient to drive P-body
286 localization, we transplanted the 3'UTR of *BSC1* or *ATP11* to a non-P-body associated transcript
287 *SEC59* and a sodium specific P-body-associated transcript *YLR042C* (Figure 5- Figure
288 Supplement 1B). None of the four chimaeras recapitulated the localization of native *BSC1* and
289 *ATP11* transcripts under stress (Figure 5- Figure Supplement 1C, 1D). Thus, although the 3'UTRs
290 are essential, they are not sufficient by themselves to drive mRNA transport into P-bodies. Most
291 likely other elements in the coding sequence and/or 5'UTR act cooperatively.

292 **Overexpression of *ATP11* rescues the glycogen accumulation deficiency in ∆*puf5* cells**

293 Finally, we asked whether the stabilization of *ATP11* mRNA by Puf5p is beneficial for the cell.
294 Puf5 promotes chronological lifespan (Stewart et al., 2007), which is dependent on the
295 accumulation of carbohydrates such as glycogen (Cao et al., 2016). Likewise, a ∆*atp11* strain
296 showed decreased glycogen accumulation (Wilson et al., 2002). Therefore, we asked whether
297 Atp11p levels would contribute to the Puf5p ability to promote lifespan and stained for glycogen
298 when cells reached stationary phase. As expected ∆*atp11* and ∆*puf5* failed to efficiently
299 accumulate glycogen as indicated by the absence of the brown color (Figure 5F). Importantly
300 overexpression of *ATP11* in the ∆*puf5* strain was sufficient to restore glycogen accumulation,
301 suggesting that the stabilization of *ATP11* mRNA by Puf5p contributes to Puf5p's positive effect
302 on chronological lifespan.
303
304
305

bioRxiv preprint doi: https://doi.org/10.1101/159376; this version posted July 4, 2017. The copyright holder for this preprint (which was not certified by peer review) is the author/funder, who has granted bioRxiv a license to display the preprint in perpetuity. It is made available under aCC-BY 4.0 International license.

306 **Discussion**

307

308 The fate of mRNAs and its regulation under different stress conditions is still not well understood.
309 mRNAs have been proposed to be either associated with ribosomes or stored/decayed in P-
310 bodies and SG. Here we demonstrate that the content and the fate of mRNA in P-bodies is stress-
311 dependent, varying from decay to stabilization. We furthermore provide evidence that different
312 mRNA classes use different mechanisms to be P-body localized. The localization and fate of
313 these mRNAs are dependent on interactions with RNA binding proteins such as Puf5p and
314 essential information present in the 3'UTR of the mRNA.

315 To enable this analysis, we first devised a method to enrich RNPs based on *in vivo*
316 chemical cross-linking followed by streptavidin affinity purification. This method allows the
317 identification and global analysis of P-body associated mRNAs. We previously used a similar
318 approach to successfully discover a novel exomer-dependent cargo (Ritz et al., 2014) and a novel
319 facultative P-body component (Weidner et al., 2014). We improved the procedure permitting the
320 reliable enrichment and detection of mRNAs associated with P-bodies under a variety of stress
321 conditions. Moreover, our method works regardless of poly(A) tail length or partial transcript
322 degradation, and hence could be applied for the identification of many types of RNAs. Moreover,
323 this method would also be applicable to study protein-DNA interactions.

324 We mostly concentrated our further analysis on hits from the glucose starvation
325 experiments but it is very likely that these findings can be generalized to other stresses. We
326 identified three classes of mRNAs in P-bodies. The first class consists of mRNAs that are
327 generally deposited into P-bodies, independent of the stressor. We did not investigate their fate
328 further in this study, but we assume that most of those transcripts would be prone to decay. The
329 second class contains mRNAs that are stressor-dependent and decayed. It is important to note
330 that the decay rate of mRNAs in this class is very variable and could represent an intrinsic property
331 of the mRNA or a subset of mRNAs. Some transcripts will be decayed almost immediately after

bioRxiv preprint doi: https://doi.org/10.1101/159376; this version posted July 4, 2017. The copyright holder for this preprint (which was not certified by peer review) is the author/funder, who has granted bioRxiv a license to display the preprint in perpetuity. It is made available under aCC-BY 4.0 International license.

332 arrival in P-bodies, while others are initially excluded from degradation. The kinetics of decay also
333 appears to vary, indicating that even within P-bodies the degradation of client RNAs is highly
334 regulated. Finally, the third class corresponds to mRNAs that are also stress-specific, but
335 stabilized, rather than degraded. It appears as if this class is enriched in transcripts whose
336 products would be beneficial for stress survival. This hypothesis is based on the stabilization of
337 transcripts involved in mitochondrial function under glucose starvation, a condition under which
338 mitochondria are up-regulated (Wu et al., 2004). Thus, P-bodies emerge as context-dependent
339 regulator in stress responses. Although P-bodies have been proposed previously as mRNA decay
340 and storage organelles (Sheth and Parker, 2003), the studies on which this model was based had
341 either been performed on very few selected transcripts or artificial transcripts with extended G-
342 tracts driving P-body localization through imaging or genome-wide analyses, taking all the mRNAs
343 present in a lysate into account (Arribere et al., 2011; Brengues et al., 2005; Sun et al., 2013).
344 Our approach is different in that we enrich first for P-bodies and then extract the RNA specifically
345 from the P-body fraction. Therefore, our data provide an unprecedented wealth of information on
346 the mRNA content and fate within P-bodies.

347 Since the fate of an mRNA is stressor-dependent, it is tempting to speculate that the
348 different mRNA classes are recruited to P-bodies through different pathways. In support of this
349 hypothesis, we identified the RNA binding protein Puf5p as a protein regulating both the
350 localization of on transcript as well as the degradation of another (Figure 6). The latter function is
351 easily explained by the established role of Puf5p as interactor of the Crr4/Not deadenylation
352 complex, which shortens the poly(A)-tail independent of the subsequent route of destruction
353 through P-bodies or exosomes (Balagopal et al., 2012). In fact, *BSC1* mRNA was recently
354 identified as Puf5p target (Wilinski et al., 2015). In the absence of Puf5p, *ATP11* is no longer P-
355 body localized and is destabilized. Hence, in this case P-bodies protect an mRNA from
356 degradation in a Puf5p-dependent manner. It is striking, however, that Puf5p possesses this dual

bioRxiv preprint doi: https://doi.org/10.1101/159376; this version posted July 4, 2017. The copyright holder for this preprint (which was not certified by peer review) is the author/funder, who has granted bioRxiv a license to display the preprint in perpetuity. It is made available under aCC-BY 4.0 International license.

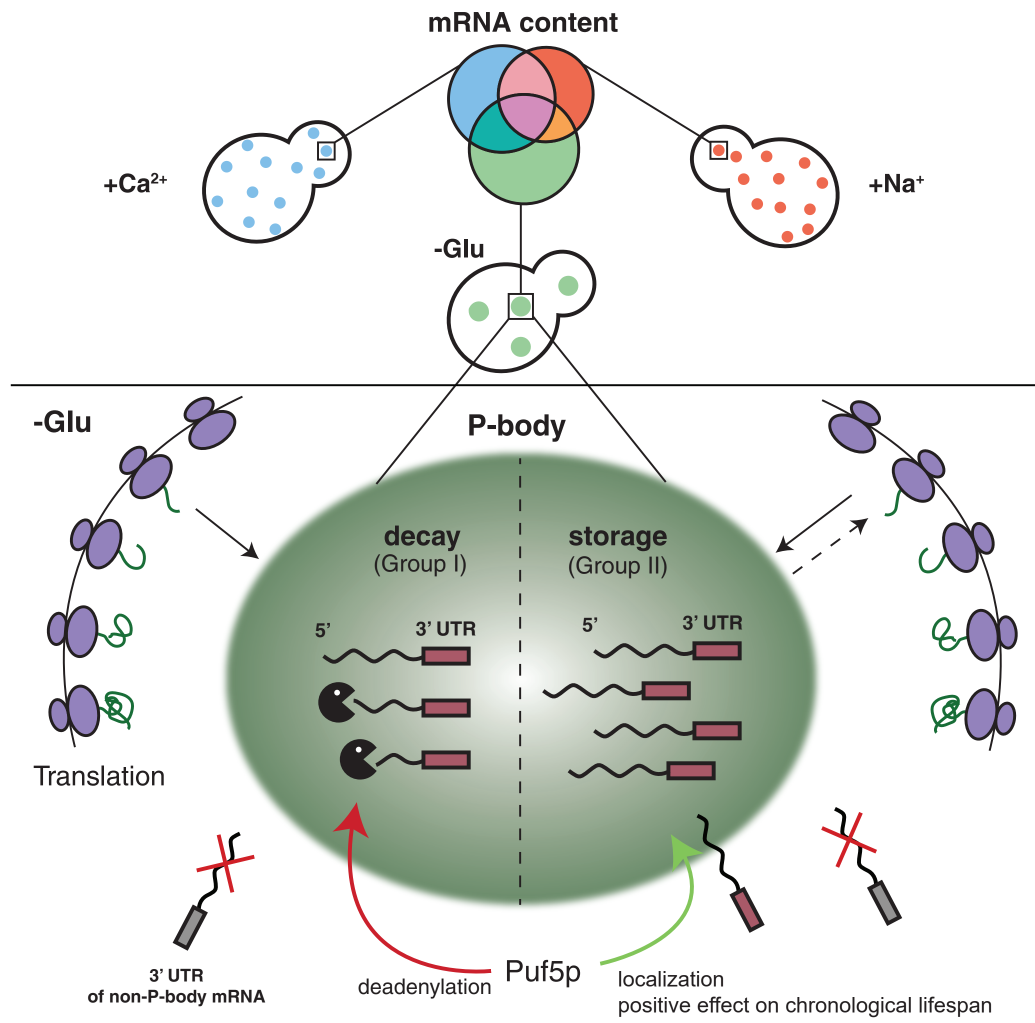

Figure 6. Schematic model summarizing our findings.

bioRxiv preprint doi: https://doi.org/10.1101/159376; this version posted July 4, 2017. The copyright holder for this preprint (which was not certified by peer review) is the author/funder, who has granted bioRxiv a license to display the preprint in perpetuity. It is made available under aCC-BY 4.0 International license.

357 role of protection and destruction depending on the mRNA, as well as being involved in the
358 localization of mRNAs to P-bodies.

359 The notion that mRNAs are decayed in P-bodies was recently challenged (Pelechano et
360 al., 2015; Sweet et al., 2012). Instead, it was suggested that decay might mostly happen co-
361 translationally. We cannot exclude that a part of the RNAs is degraded co-translationally, since
362 the decay machinery in both processes appears to be identical. In favor of mRNA decay in P-
363 bodies, we confirmed hits from the biochemical enrichment procedure by *in vivo* localization
364 studies. We found that P-body-localized mRNAs were degraded with different kinetics. Moreover,
365 we would expect to find significantly higher sequence coverage of the 3' region of candidate
366 mRNAs, which we did not observe. Also, the fate -stabilization versus degradation- of *BSC1* in a
367 Puf5p-dependent manner, which was not accompanied by modulating P-body localization, is in
368 support of P-body as decay compartment. Thus, our data are consistent with mRNA degradation
369 in P-bodies under stress conditions. In contrast, *ATP11* may become a co-translational
370 degradation target in the absence of Puf5p. However co-translational mRNA decay might still be
371 a major pathway in non-stressed cells, in which microscopically P-bodies are not frequently
372 detected. At least the 5' decay machinery, the helicase Dhh1p and the 5'exonuclease Xrn1p have
373 been found to be associated with polysomes also in the absence of a stressor (Pelechano et al.,
374 2015; Sweet et al., 2012; Weidner et al., 2014).

375 Our findings demonstrate that P-body associated mRNA can follow different fates, namely
376 decay or stabilization. Whether these two functions are performed by the same or different P-
377 bodies remains unclear. We favor the possibility, however, that both functions can be provided by
378 the same P-body. Recent data from *Drosophila* sponge bodies, which are the equivalent of P-
379 bodies in embryos, suggest that the degradation and decay may happen in the same
380 compartment (Weil et al., 2012). Likewise, there is no evidence thus far for differential protein
381 composition of P-bodies formed under the same stress condition (Kulkarni et al., 2010). Although,

bioRxiv preprint doi: https://doi.org/10.1101/159376; this version posted July 4, 2017. The copyright holder for this preprint (which was not certified by peer review) is the author/funder, who has granted bioRxiv a license to display the preprint in perpetuity. It is made available under aCC-BY 4.0 International license.

382 it is possible that the transient protein components may vary from one another, we expect the
383 major factors would be discriminative to fulfill opposing functions and mRNA selectivity.
384 Stabilized mRNAs may return into the translation competent pool. Whether this re-initiation
385 would be through diffusion of the mRNA from the P-body into the cytoplasm or through another
386 organelle, such as stress granules (SG), remains to be established. SGs harbor stalled translation
387 initiation complexes, whose formation can also be triggered upon a variety of stresses.
388 Additionally, SGs frequently dock and fuse with P-bodies, and they share some common protein
389 factors (Buchan et al., 2008; Buchan et al., 2011; Kedersha et al., 2005; Stoecklin and Kedersha,
390 2013). As mRNAs in SGs are polyadenylated, they are not subject to immediate degradation
391 (Kedersha et al., 1999; Stoecklin and Kedersha, 2013). Based on those evidences, we speculate
392 that the re-engagement of stable transcripts into translation is likely mediated via SGs.
393 A number of genome-wide studies detailing responses to stress have been performed
394 (Miller et al., 2011; Munchel et al., 2011). Most of the studies deal with global RNA synthesis and
395 decay, but do not provide any insights into the regulated storage of mRNA. In this study, we
396 addressed this issue and uncovered Puf5 as key molecule in the decision making whether or not
397 a particular mRNA must be degraded under glucose starvation. This decision making explains
398 Puf5p's positive effect on chronological lifespan, as increasing Atp11p levels were sufficient to
399 rescue the glycogen accumulation defect of Δ*puf5* cells. How the decision making is brought about
400 will be the focus of future studies.
401
402
403
404
405
406
407

bioRxiv preprint doi: https://doi.org/10.1101/159376; this version posted July 4, 2017. The copyright holder for this preprint (which was not certified by peer review) is the author/funder, who has granted bioRxiv a license to display the preprint in perpetuity. It is made available under aCC-BY 4.0 International license.

408 **Materials and Methods**

409 **Yeast strains and growth conditions**

410 Standard genetic techniques were employed throughout (Sherman, 1991). Unless otherwise
411 noted, all genetic modifications were carried out chromosomally. Chromosomal tagging and
412 deletions were performed as described (Janke et al., 2004; Knop et al., 1999). For C-terminal
413 tagging with 3xHA, the plasmid pYM-3HA (*klTRP1*) and with 9xmyc the plasmid pOM20 (*kanMX6*)
414 and pSH47 (*URA3*) were used. The use of pOM plasmids (Gauss et al., 2005) in combination
415 with Cre recombinase allowed C-terminal chromosomal tagging and preservation of the
416 endogenous 3'UTR at the same time. The plasmid pFA6a-natNT2 was used for construction of
417 all deletion strains, except for *Δpuf3* (pUG73), Δ*atp11* and Δ*bsc1* (pUG72). 3'UTR transplantation
418 experiments were carried out with the *Delitto Perfetto* method using the pCORE plasmid
419 (*kanMX4-URA3*) (Storici and Resnick, 2006).

420 For C-terminal tagging Puf5p with GFP, the plasmid pYM26 (*klTRP1*) was used. pFA6a-
421 3xmcherry (*hphNT1*) plasmid was used in tagging Dcp2p with mcherry (Maeder et al., 2007). For
422 live-cell mRNA imaging, MS2SL tagged strains were constructed using pDZ415 (24MS2SL loxP-
423 Kan-loxP). To remove selection marker and visualize the transcripts, the Cre recombinase-
424 containing plasmid pSH47 (URA3) and MS2SL coat protein expressing plasmid pDZ274 (pLEU
425 MET25pro MCP-2x-yeGFP) were co-transformed into cells afterwards (Hocine et al., 2013).
426 Plasmids pDZ415 (Addgene plasmid # 45162) and pDZ274 (Addgene plasmid # 45929) were
427 gifts from Robert Singer and Daniel Zenklusen (Albert Einstein College of Medicine, Bronx, NY,
428 USA). Primers and strains used in this study are listed in Table S3 and S4.

429 Unless otherwise noted, yeast cells were grown in YPD (1% yeast extract, 2% peptone,
430 2% dextrose) at 30˚C. For glucose deprivation, cultures were further grown in YP media without
431 dextrose for indicated times. For mild osmotic stress, YPD growth medium was supplemented
432 with 0.5 M NaCl or 0.2 M $CaCl_2$ for indicated times. Yeast cells were harvested at mid-log phase
433 (OD_{600} of 0.4-0.8).

bioRxiv preprint doi: https://doi.org/10.1101/159376; this version posted July 4, 2017. The copyright holder for this preprint (which was not certified by peer review) is the author/funder, who has granted bioRxiv a license to display the preprint in perpetuity. It is made available under aCC-BY 4.0 International license.

434 **Chemical cross-linking coupled to affinity Purification (cCLAP) and preparation of RNA-**
435 **Seq samples**

436 The cCLAP was carried out according to Tagwerker et al. (2006), Hafner et al. (2010) and Kishore
437 et al. (2011) with modifications. Cells expressing Dcp2-HBH or Scd6-HBH were grown to mid-log
438 phase, subjected to the corresponding stress and crosslinked with 1% formaldehyde for 2 min.
439 Control cells were treated equally except stress application. Cells were lysed in RIPA buffer
440 (50 mM Tris-HCl pH 8.0, 150 mM NaCl, 1% NP-40, 0.5% sodium deoxycholate, 0.1% SDS,
441 supplemented with protease inhibitors) using FastPrep (MP Biomedicals). To dissolve large RNPs,
442 supernatants were treated with 50 U/ml RNase T1 (Fermentas) at 22°C for 15 min. Pull-downs
443 were performed with streptavidin agarose beads (Thermo Fisher Scientific) in binding buffer
444 (50 mM NaPi pH 8.0, 300 mM NaCl, 6 M GuHCl, 0.5% Tween-20). The second RNase T1
445 digestion was performed on the beads with a final concentration of 1 U/µl. Radiolabeling of RNA
446 was performed by adding 0.5 µCi/µl γ-^{32}P-ATP (Hartmann analytic) and 1 U/µl T4 PNK (New
447 England Biolabs). To purify RNA, proteins were digested using 1.2 mg/ml proteinase K (Roche)
448 in 2 x proteinase K buffer (100 mM Tris-HCl pH 7.5, 200 mM NaCl, 2 mM EDTA, 1% SDS) for
449 30 min at 55˚C. The RNA was subsequently isolated using phenol-chloroform-isoamyl alcohol
450 (125:24:1) (Sigma-Aldrich) as described (Schmitt et al., 1990). Purified RNA was subjected to 3’
451 and 5’ adapter ligation following Illumina’s TruSeq Small RNA Library Prep Guide. To reduce the
452 rRNA species, RiboMinus transcriptome isolation kit (Invitrogen) was used according to the
453 manufacturer's protocol. Reverse transcription using SuperScript III reverse transcriptase
454 (Invitrogen), oligo-dT and random hexamer was performed afterwards. The cDNA libraries were
455 generated by a final PCR amplification step with Ilumina indexing primer (RPI1-4, Table S2).
456 In this study, five library sets (from five biological replicates) were sequenced. Except the first
457 library set, all the libraries were generated as described above. In the first library set, the
458 radiolabeling step was omitted and the PAGE purification steps were replaced by column-based
459 purification with RNeasy kit (Qiagen), according to the manufacturer’s instruction.

bioRxiv preprint doi: https://doi.org/10.1101/159376; this version posted July 4, 2017. The copyright holder for this preprint (which was not certified by peer review) is the author/funder, who has granted bioRxiv a license to display the preprint in perpetuity. It is made available under aCC-BY 4.0 International license.

460 **Processing of small RNA-Seq reads**

461 RNA-Seq libraries were sequenced on Illumina HiSeq2000 with single read to 50 bp reads. We
462 clipped adapters and trimmed low quality bases using Trimmomatic version 0.30 (Bolger et al.,
463 2014) with parameters “SE –s phred33 ILLUMINACLIP:Illumina_smallRNA_adapters.fa:20:5:30
464 LEADING:30 TRAILING:30 MINLEN:10”, where Illumina_smallRNA_adapters.fa contained all
465 adapter and primer sequences from the TruSeq Small RNA Sample Preparation Kit.
466 Subsequently, reads were aligned to Saccharomyces cerevisiae genome EF4.72 from ENSEMBL
467 using Bowtie version 1.0.0 (Langmead et al., 2009) with parameters “-n 0 –l 28 –e 70 –k1 –m 1 -
468 -best --strata --sam --nomaqround”. Reads were counted per exon using htseq-count (Anders et
469 al., 2015) with default parameters against ENSEMBL’s matching GTF file for EF4.72 and
470 aggregated on the gene-level.

471 **Analysis of P-body enriched mRNAs**

472 Analysis of P-body enriched mRNAs was performed using edgeR version 3.0 (Robinson et al.,
473 2010) using standard procedures for count normalization and estimation of dispersion. The gel
474 label and batch were included as factors in the experimental design (Table S5). We identified
475 significant (p<0.05) upregulated mRNAs exclusive for each stress condition by testing each
476 individual stress condition against the wild type condition and removing those mRNAs that were
477 identified as common hits when testing the joint set of stress conditions against unstressed control.
478 For glucose depletion stress, we additionally excluded genes previously shown to be significantly
479 enriched in polysomes (Arribere et al., 2011) for the same stress.

480 **Gene Ontology (GO) term enrichment analysis**

481 P-body enriched mRNAs for each stress condition were tested for GO biological processes (BP)
482 enrichment using hypergeometric tests as implemented in the hyperGTest function from the
483 GOstats R/Bioconductor package version 1.7.4. The mRNA universe was defined for each stress
484 condition as the set of mRNAs with a mean expression over all replicates larger than or equal to
485 the first quartile. For GO term mRNA annotation, the R/Bioconductor package org.Sc.sgd.db

bioRxiv preprint doi: https://doi.org/10.1101/159376; this version posted July 4, 2017. The copyright holder for this preprint (which was not certified by peer review) is the author/funder, who has granted bioRxiv a license to display the preprint in perpetuity. It is made available under aCC-BY 4.0 International license.

486 version 3.1.2 was used. P-values from the hypergeometric tests were visualized using the ggplot2
487 R package version 1.0.1.

488 **Combined fluorescence in situ hybridization (FISH) and immunofluorescence (IF)**

489 Combined FISH and IF was performed as described (Kilchert et al., 2010; Takizawa et al., 1997).
490 The following antibodies and solution were used for detection: anti-DIG-POD (Roche, 1:750 in
491 PBTB), anti-HA (Eurogentec HA11; 1:250), anti-GFP (Roche GFP clones 7.1 and 13.1, 1:250),
492 goat anti-mouse-IgG-Alexa488 (Invitrogen, 1:400 in PBS) and tyramide solution (PerkinElmer,
493 1:100 in Amplification Solution supplied with kit). Primers with T7 promoter ends (Table S3) and
494 MEGAscript T7 transcription kit (Ambion) were used for probe generation. To obtain fluorescence
495 images, slides were mounted with Citifluor AF1 (Citifluor), supplemented with 1 µg/ml DAPI to
496 stain the nuclei. Images were acquired with an Axiocam MRm camera mounted on an Axioplan 2
497 fluorescence microscope using a Plan Apochromat 63x/NA1.40 objective and filters for eqFP611
498 and GFP. Axiovision software 3.1 to 4.8 was used to process images (Carl Zeiss).

499 **Co-localization analysis**

500 Signals of P-bodies and mRNA were identified using the spots tools in Imaris software package
501 (Bitplane). For co-localization determination, the MATLAB (MathWorks)- Imaris plug-in "co-
502 localize spots" function was used with a threshold of 50% of the distance between centers of two
503 spots. The percentage of mRNA co-localization with P-bodies was calculated by dividing co-
504 localized FISH spots by total FISH spots. Approximately 200 cells from at least three biologically
505 independent experiments were counted per mRNA per condition.

506 **Pulse-chase labeling with 4TU and RNA purification**

507 The pulse-chase labeling experiment was carried out as described previously (Zeiner et al., 2008).
508 For the pulse, yeast culture was grown in HC-Ura drop-out media supplemented with 2% dextrose,
509 0.1 mM uracil and 0.2 mM 4-Thiouracil (Sigma-Aldrich) for 6 h. Yeast were spun down at 3,000 g
510 for 2 min and resuspended in HC-Ura drop-out media containing 20 mM uracil (chase).
511 Afterwards, yeasts were collected by centrifugation at the following time points: t = 0, 10, 20, 30,

bioRxiv preprint doi: https://doi.org/10.1101/159376; this version posted July 4, 2017. The copyright holder for this preprint (which was not certified by peer review) is the author/funder, who has granted bioRxiv a license to display the preprint in perpetuity. It is made available under aCC-BY 4.0 International license.

512 and 60 min. Cells were lysed followed by total RNA isolation using phenol-chloroform-isoamyl
513 alcohol (125:24:1) (Sigma-Aldrich) as described (Schmitt et al., 1990). The RNA was then
514 subjected to biotinylation and further purification according to Zeiner et al. (2008).

515 The same pulse-chase labeling protocol was performed to determine the mRNA stability
516 of *ACT1*, *PGK1* and *RPL37b* under glucose deprivation condition, and 200 pg humanized Renilla
517 luciferase (*hRLuc*) RNA spike-in was added per microgram total RNA as reference gene. The
518 same RNA purification protocol was followed to isolate 4TU labeled RNA as well as total RNA. At
519 least three biologically independent pulse-chase experiments per mRNA per strain were
520 performed.

521 **Quantitative RT-PCR**

522 0.5-1 μg of 4-TU labeled RNA or total RNA was reverse transcribed with the Transcriptor reverse
523 transcriptase kit (Roche), oligo-dTs and random hexamers. The mRNA levels were analyzed by
524 SYBR green incorporation using ABI StepOne Plus real-time PCR system (Applied Biosystems).
525 Primers used in qRT-PCR are listed in Table S3.

526 **Western Blotting**

527 Glucose deprived cells were harvested at indicated times. For each time point, 9 ml of culture was
528 collected, immediately treated with cold trichloroacetic acid (10% final concentration), and
529 incubated on ice for 5 min. Yeast extracts were prepared as described (Stracka et al., 2014). The
530 protein concentration was determined using the DC Protein Assay (Bio-Rad), and the total lysate
531 was analyzed by SDS-PAGE and immunoblotting. The following antibodies were used for
532 immunoblotting: anti-Tpi1p (LSBio LS-C147665; 1:5,000); anti-Atp11p (a gift from Sharon H.
533 Ackerman, Wayne State University, Detroit, MI); anti-HA (Eurogentec HA11; 1:1,000); anti-myc
534 (M4439; Sigma-Aldrich; 1:1,000); anti-Pgk1p (Invitrogen #A-6457; 1:1,000). Enhanced
535 Chemiluminescence (ECL; GE Healthcare) was used for detection.

536

537

bioRxiv preprint doi: https://doi.org/10.1101/159376; this version posted July 4, 2017. The copyright holder for this preprint (which was not certified by peer review) is the author/funder, who has granted bioRxiv a license to display the preprint in perpetuity. It is made available under aCC-BY 4.0 International license.

538 **Live-cell imaging**

539 For live-cell imaging with MS2 system. Yeast cells were grown in HC-Leu medium containing 2%
540 glucose to mid-log phase. The cells were taken up in glucose-free HC-Leu medium afterwards.
541 For live-cell imaging with Dcp2p and Pufp, Yeast cells were grown in YPD medium to mid-log
542 phase, and resuspended in HC-complete medium lacking glucose. Fluorescence was monitored
543 as described in FISH-IF.

544 **Electrophoretic mobility shift assays (EMSA)**

545 Recombinant GST-PUF3 (amino acids 465-879) and GST-PUF5 (amino acids 126–626)
546 expressed form pWO12 and pWO18 (Gifts from Wendy M. Olivas, University of Missouri St. Louis,
547 St. Louis, MO), respectively were purified and stored in 50mM Tris/HCl pH 8.0, 10% glycerol. The
548 *ATP11* 3'UTR RNA (1-500 nt after STOP codon) was transcribed from a template containing T7
549 RNA polymerase promoter with MEGAscript T7 transcription kit (Ambion) and α-^{32}P-UTP
550 (10mCi/ml). Binding reactions (20 μL) contained 4,000 cpm of labelled RNA, varying
551 concentrations of protein, 20 U RNasin Plus RNase Inhibitor (Promega) and 1 x binding buffer
552 (10 mM Tris/HCl pH 7.5, 100 mM KCl, 1 mM EDTA, 0.1 mM DTT, 0.01 mg/ml bovine serum
553 albumin, 5% glycerol). Reactions were incubated at RT for 30 min, and separated on a 4% non-
554 denaturing acrylamide gel. Gels were dried, exposed to a phosphor screen for 10-16 hours, and
555 the screens scanned using a phosphorimager (Typhoon FLA 7000, GE Healthcare).

556 **Identification of secondary structure motifs within the 3'UTRs of P-Body-associated**
557 **mRNAs**

558 Secondary structure motifs in the 3' untranslated regions (UTRs) of transcripts, overrepresented
559 among differentially enriched mRNAs for each stress condition, were identified using NoFold
560 (Middleton and Kim, 2014) version 1.0. 3' UTR sequences were extracted from the biomart
561 (http://biomart.org) by selecting 300 base pairs (bp) downstream of the coding sequence (CDS).
562 The internal NoFold boundary file bounds_300seq.txt was used along with a file containing UTR

bioRxiv preprint doi: https://doi.org/10.1101/159376; this version posted July 4, 2017. The copyright holder for this preprint (which was not certified by peer review) is the author/funder, who has granted bioRxiv a license to display the preprint in perpetuity. It is made available under aCC-BY 4.0 International license.

563 sequences of all non-enriched mRNAs as a background for enrichment analysis and parameter -
564 -rnaz. All other parameters were used in the default setting.

565 **Analysis of intracellular glycogen**

566 Glycogen content in yeast cells was visualized using iodine staining (Quain and Tubb, 1983). Wild
567 type, Dcp2-GFP Δ*atp11,* Dcp2-GFP Δ*puf5* and Dcp2-GFP Δ*bsc1* strains were grown in HC
568 medium, and strains containing the *ATP11* overexpression plasmid were grown in HC-Ura
569 medium. All strains allowed to reach stationary phase (OD_{600} ~2.4) and subsequently shifted for
570 1 hr to medium lacking glucose. Samples were taken before and after dextrose depletion, iodine
571 (Sigma-Aldrich) was added to a final concentration of 0.5 mg/ml iodine. The intensities of
572 produced yellow-brown stain positively correlate with their intracellular glycogen levels.

573 **Accession Numbers**

574 The RNA-Seq data reported in this study is deposited in Gene Expression Omnibus (GEO)
575 database, and the accession number is GSE76444.

bioRxiv preprint doi: https://doi.org/10.1101/159376; this version posted July 4, 2017. The copyright holder for this preprint (which was not certified by peer review) is the author/funder, who has granted bioRxiv a license to display the preprint in perpetuity. It is made available under aCC-BY 4.0 International license.

576 **Acknowledgements**

577 We thank C. Brown, M. Zavolan and J. Guimaraes for help with the data analysis and discussions,
578 and M. Zavolan, I. G. Macara, T. Gross, R. P. Jansen and W. Filipowicz for critical comments on
579 the manuscript. S. Ackerman and W. Olivas are acknowledged for providing the Atp11 antibody
580 and the *PUF3* and *PUF5* constructs, respectively. This work was supported through grants from
581 HFSP (RGP0031), the Swiss National Science Foundation (31003A_141207, 310030B_163480)
582 and the University of Basel to AS. CW and JW were supported by Werner Siemens Fellowships
583 and FS by SystemsX.ch (2009/025), the Swiss Initiative in Systems Biology.

584

585 **Author Contributions**

586 AS and CW conceived the project and experiments. Most experiments were performed by CW.
587 JW was involved in initial experiments. FS, CW, NB and AS performed data analysis. AS, CW
588 and FS wrote the manuscript with input from all authors.

589

590 **Financial competing interests**

591 The authors declare no competing financial interests.

592

593 **Materials & Correspondence**

594 Correspondence to: Anne Spang (anne.spang@unibas.ch).

595

596

597

598

599

600

bioRxiv preprint doi: https://doi.org/10.1101/159376; this version posted July 4, 2017. The copyright holder for this preprint (which was not certified by peer review) is the author/funder, who has granted bioRxiv a license to display the preprint in perpetuity. It is made available under aCC-BY 4.0 International license.

601 **Reference**

602 Anders, S., Pyl, P.T., and Huber, W. (2015). HTSeq--a Python framework to work with high-
603 throughput sequencing data. Bioinformatics 31, 166-169.
604 Anderson, J.S., and Parker, R.P. (1998). The 3' to 5' degradation of yeast mRNAs is a general
605 mechanism for mRNA turnover that requires the SKI2 DEVH box protein and 3' to 5'
606 exonucleases of the exosome complex. The EMBO journal 17, 1497-1506.
607 Andreassi, C., and Riccio, A. (2009). To localize or not to localize: mRNA fate is in 3'UTR ends.
608 Trends in cell biology 19, 465-474.
609 Arribere, J.A., Doudna, J.A., and Gilbert, W.V. (2011). Reconsidering movement of eukaryotic
610 mRNAs between polysomes and P bodies. Molecular cell 44, 745-758.
611 Ashe, M.P., De Long, S.K., and Sachs, A.B. (2000). Glucose depletion rapidly inhibits
612 translation initiation in yeast. Molecular biology of the cell 11, 833-848.
613 Bailey, T.L., Boden, M., Buske, F.A., Frith, M., Grant, C.E., Clementi, L., Ren, J., Li, W.W., and
614 Noble, W.S. (2009). MEME SUITE: tools for motif discovery and searching. Nucleic Acids Res
615 37, W202-208.
616 Balagopal, V., Fluch, L., and Nissan, T. (2012). Ways and means of eukaryotic mRNA decay.
617 Biochimica et biophysica acta 1819, 593-603.
618 Bolger, A.M., Lohse, M., and Usadel, B. (2014). Trimmomatic: a flexible trimmer for Illumina
619 sequence data. Bioinformatics 30, 2114-2120.
620 Brengues, M., Teixeira, D., and Parker, R. (2005). Movement of eukaryotic mRNAs between
621 polysomes and cytoplasmic processing bodies. Science 310, 486-489.
622 Buchan, J.R., Muhlrad, D., and Parker, R. (2008). P bodies promote stress granule assembly in
623 Saccharomyces cerevisiae. The Journal of cell biology 183, 441-455.
624 Buchan, J.R., Yoon, J.H., and Parker, R. (2011). Stress-specific composition, assembly and
625 kinetics of stress granules in Saccharomyces cerevisiae. Journal of cell science 124, 228-239.

bioRxiv preprint doi: https://doi.org/10.1101/159376; this version posted July 4, 2017. The copyright holder for this preprint (which was not certified by peer review) is the author/funder, who has granted bioRxiv a license to display the preprint in perpetuity. It is made available under aCC-BY 4.0 International license.

626 Cai, Y., and Futcher, B. (2013). Effects of the yeast RNA-binding protein Whi3 on the half-life
627 and abundance of CLN3 mRNA and other targets. PloS one 8, e84630.
628 Cao, L., Tang, Y., Quan, Z., Zhang, Z., Oliver, S.G., and Zhang, N. (2016). Chronological
629 Lifespan in Yeast Is Dependent on the Accumulation of Storage Carbohydrates Mediated by
630 Yak1, Mck1 and Rim15 Kinases. PLoS genetics 12, e1006458.
631 Chritton, J.J., and Wickens, M. (2010). Translational repression by PUF proteins in vitro. Rna
632 16, 1217-1225.
633 Chung, S., and Takizawa, P.A. (2011). In vivo visualization of RNA using the U1A-based tagged
634 RNA system. Methods Mol Biol 714, 221-235.
635 Davidson, A., Parton, R.M., Rabouille, C., Weil, T.T., and Davis, I. (2016). Localized Translation
636 of gurken/TGF-alpha mRNA during Axis Specification Is Controlled by Access to Orb/CPEB on
637 Processing Bodies. Cell reports 14, 2451-2462.
638 Decker, C.J., and Parker, R. (2012). P-bodies and stress granules: possible roles in the control
639 of translation and mRNA degradation. Cold Spring Harbor perspectives in biology 4, a012286.
640 Garcia, J.F., and Parker, R. (2015). MS2 coat proteins bound to yeast mRNAs block 5' to 3'
641 degradation and trap mRNA decay products: implications for the localization of mRNAs by MS2-
642 MCP system. Rna 21, 1393-1395.
643 Gauss, R., Trautwein, M., Sommer, T., and Spang, A. (2005). New modules for the repeated
644 internal and N-terminal epitope tagging of genes in Saccharomyces cerevisiae. Yeast 22, 1-12.
645 Gerber, A.P., Herschlag, D., and Brown, P.O. (2004). Extensive association of functionally and
646 cytotopically related mRNAs with Puf family RNA-binding proteins in yeast. PLoS biology 2,
647 E79.
648 Goldstrohm, A.C., Hook, B.A., Seay, D.J., and Wickens, M. (2006). PUF proteins bind Pop2p to
649 regulate messenger RNAs. Nat Struct Mol Biol 13, 533-539.
650 Hafner, M., Landthaler, M., Burger, L., Khorshid, M., Hausser, J., Berninger, P., Rothballer, A.,
651 Ascano, M., Jr., Jungkamp, A.C., Munschauer, M., et al. (2010). Transcriptome-wide

bioRxiv preprint doi: https://doi.org/10.1101/159376; this version posted July 4, 2017. The copyright holder for this preprint (which was not certified by peer review) is the author/funder, who has granted bioRxiv a license to display the preprint in perpetuity. It is made available under aCC-BY 4.0 International license.

652 identification of RNA-binding protein and microRNA target sites by PAR-CLIP. Cell 141, 129-
653 141.
654 Hey, F., Czyzewicz, N., Jones, P., and Sablitzky, F. (2012). DEF6, a novel substrate for the Tec
655 kinase ITK, contains a glutamine-rich aggregation-prone region and forms cytoplasmic granules
656 that co-localize with P-bodies. J Biol Chem 287, 31073-31084.
657 Hocine, S., Raymond, P., Zenklusen, D., Chao, J.A., and Singer, R.H. (2013). Single-molecule
658 analysis of gene expression using two-color RNA labeling in live yeast. Nature methods 10,
659 119-121.
660 Huch, S., Gommlich, J., Muppavarapu, M., Beckham, C., and Nissan, T. (2016). Membrane-
661 association of mRNA decapping factors is independent of stress in budding yeast. Scientific
662 reports 6, 25477.
663 Janke, C., Magiera, M.M., Rathfelder, N., Taxis, C., Reber, S., Maekawa, H., Moreno-Borchart,
664 A., Doenges, G., Schwob, E., Schiebel, E., et al. (2004). A versatile toolbox for PCR-based
665 tagging of yeast genes: new fluorescent proteins, more markers and promoter substitution
666 cassettes. Yeast 21, 947-962.
667 Kedersha, N., Stoecklin, G., Ayodele, M., Yacono, P., Lykke-Andersen, J., Fritzler, M.J.,
668 Scheuner, D., Kaufman, R.J., Golan, D.E., and Anderson, P. (2005). Stress granules and
669 processing bodies are dynamically linked sites of mRNP remodeling. J Cell Biol 169, 871-884.
670 Kedersha, N.L., Gupta, M., Li, W., Miller, I., and Anderson, P. (1999). RNA-binding proteins TIA-
671 1 and TIAR link the phosphorylation of eIF-2 alpha to the assembly of mammalian stress
672 granules. The Journal of cell biology 147, 1431-1442.
673 Kilchert, C., Weidner, J., Prescianotto-Baschong, C., and Spang, A. (2010). Defects in the
674 secretory pathway and high Ca2+ induce multiple P-bodies. Mol Biol Cell 21, 2624-2638.
675 Kishore, S., Jaskiewicz, L., Burger, L., Hausser, J., Khorshid, M., and Zavolan, M. (2011). A
676 quantitative analysis of CLIP methods for identifying binding sites of RNA-binding proteins.
677 Nature methods 8, 559-564.

bioRxiv preprint doi: https://doi.org/10.1101/159376; this version posted July 4, 2017. The copyright holder for this preprint (which was not certified by peer review) is the author/funder, who has granted bioRxiv a license to display the preprint in perpetuity. It is made available under aCC-BY 4.0 International license.

678 Knop, M., Siegers, K., Pereira, G., Zachariae, W., Winsor, B., Nasmyth, K., and Schiebel, E.
679 (1999). Epitope tagging of yeast genes using a PCR-based strategy: more tags and improved
680 practical routines. Yeast 15, 963-972.
681 Kulkarni, M., Ozgur, S., and Stoecklin, G. (2010). On track with P-bodies. Biochemical Society
682 transactions 38, 242-251.
683 Langmead, B., Trapnell, C., Pop, M., and Salzberg, S.L. (2009). Ultrafast and memory-efficient
684 alignment of short DNA sequences to the human genome. Genome biology 10, R25.
685 Lavut, A., and Raveh, D. (2012). Sequestration of highly expressed mRNAs in cytoplasmic
686 granules, P-bodies, and stress granules enhances cell viability. PLoS genetics 8, e1002527.
687 Ling, Y.H., Wong, C.C., Li, K.W., Chan, K.M., Boukamp, P., and Liu, W.K. (2014). CCHCR1
688 interacts with EDC4, suggesting its localization in P-bodies. Exp Cell Res 327, 12-23.
689 Liu, J., Valencia-Sanchez, M.A., Hannon, G.J., and Parker, R. (2005). MicroRNA-dependent
690 localization of targeted mRNAs to mammalian P-bodies. Nature cell biology 7, 719-723.
691 Maeder, C.I., Hink, M.A., Kinkhabwala, A., Mayr, R., Bastiaens, P.I., and Knop, M. (2007).
692 Spatial regulation of Fus3 MAP kinase activity through a reaction-diffusion mechanism in yeast
693 pheromone signalling. Nature cell biology 9, 1319-1326.
694 Mager, W.H., and Ferreira, P.M. (1993). Stress response of yeast. The Biochemical journal 290
695 (Pt 1), 1-13.
696 Middleton, S.A., and Kim, J. (2014). NoFold: RNA structure clustering without folding or
697 alignment. Rna 20, 1671-1683.
698 Miller, C., Schwalb, B., Maier, K., Schulz, D., Dumcke, S., Zacher, B., Mayer, A., Sydow, J.,
699 Marcinowski, L., Dolken, L., et al. (2011). Dynamic transcriptome analysis measures rates of
700 mRNA synthesis and decay in yeast. Mol Syst Biol 7, 458.
701 Mitchell, S.F., Jain, S., She, M., and Parker, R. (2013). Global analysis of yeast mRNPs. Nature
702 structural & molecular biology 20, 127-133.

bioRxiv preprint doi: https://doi.org/10.1101/159376; this version posted July 4, 2017. The copyright holder for this preprint (which was not certified by peer review) is the author/funder, who has granted bioRxiv a license to display the preprint in perpetuity. It is made available under aCC-BY 4.0 International license.

703 Munchel, S.E., Shultzaberger, R.K., Takizawa, N., and Weis, K. (2011). Dynamic profiling of
704 mRNA turnover reveals gene-specific and system-wide regulation of mRNA decay. Molecular
705 biology of the cell 22, 2787-2795.
706 Pelechano, V., Wei, W., and Steinmetz, L.M. (2015). Widespread Co-translational RNA Decay
707 Reveals Ribosome Dynamics. Cell 161, 1400-1412.
708 Quain, D.E., and Tubb, R.S. (1983). A Rapid and Simple Method for the Determination of
709 Glycogen in Yeast. J I Brewing 89, 38-40.
710 Ritz, A.M., Trautwein, M., Grassinger, F., and Spang, A. (2014). The prion-like domain in the
711 exomer-dependent cargo Pin2 serves as a trans-Golgi retention motif. Cell reports 7, 249-260.
712 Robinson, M.D., McCarthy, D.J., and Smyth, G.K. (2010). edgeR: a Bioconductor package for
713 differential expression analysis of digital gene expression data. Bioinformatics 26, 139-140.
714 Schmitt, M.E., Brown, T.A., and Trumpower, B.L. (1990). A rapid and simple method for
715 preparation of RNA from Saccharomyces cerevisiae. Nucleic acids research 18, 3091-3092.
716 Sen, G.L., and Blau, H.M. (2005). Argonaute 2/RISC resides in sites of mammalian mRNA
717 decay known as cytoplasmic bodies. Nature cell biology 7, 633-636.
718 Sherman, F. (1991). Getting started with yeast. Methods Enzymol 194, 3-21.
719 Sheth, U., and Parker, R. (2003). Decapping and decay of messenger RNA occur in
720 cytoplasmic processing bodies. Science 300, 805-808.
721 Souquere, S., Mollet, S., Kress, M., Dautry, F., Pierron, G., and Weil, D. (2009). Unravelling the
722 ultrastructure of stress granules and associated P-bodies in human cells. Journal of cell science
723 122, 3619-3626.
724 Stewart, M.S., Krause, S.A., McGhie, J., and Gray, J.V. (2007). Mpt5p, a stress tolerance- and
725 lifespan-promoting PUF protein in Saccharomyces cerevisiae, acts upstream of the cell wall
726 integrity pathway. Eukaryotic cell 6, 262-270.
727 Stoecklin, G., and Kedersha, N. (2013). Relationship of GW/P-bodies with stress granules.
728 Advances in experimental medicine and biology 768, 197-211.

bioRxiv preprint doi: https://doi.org/10.1101/159376; this version posted July 4, 2017. The copyright holder for this preprint (which was not certified by peer review) is the author/funder, who has granted bioRxiv a license to display the preprint in perpetuity. It is made available under aCC-BY 4.0 International license.

729 Storici, F., and Resnick, M.A. (2006). The delitto perfetto approach to in vivo site-directed
730 mutagenesis and chromosome rearrangements with synthetic oligonucleotides in yeast.
731 Methods Enzymol 409, 329-345.
732 Stracka, D., Jozefczuk, S., Rudroff, F., Sauer, U., and Hall, M.N. (2014). Nitrogen source
733 activates TOR (target of rapamycin) complex 1 via glutamine and independently of Gtr/Rag
734 proteins. The Journal of biological chemistry 289, 25010-25020.
735 Sun, M., Schwalb, B., Pirkl, N., Maier, K.C., Schenk, A., Failmezger, H., Tresch, A., and
736 Cramer, P. (2013). Global analysis of eukaryotic mRNA degradation reveals Xrn1-dependent
737 buffering of transcript levels. Molecular cell 52, 52-62.
738 Sweet, T., Kovalak, C., and Coller, J. (2012). The DEAD-box protein Dhh1 promotes decapping
739 by slowing ribosome movement. PLoS biology 10, e1001342.
740 Tagwerker, C., Flick, K., Cui, M., Guerrero, C., Dou, Y., Auer, B., Baldi, P., Huang, L., and
741 Kaiser, P. (2006). A tandem affinity tag for two-step purification under fully denaturing
742 conditions: application in ubiquitin profiling and protein complex identification combined with in
743 vivocross-linking. Mol Cell Proteomics 5, 737-748.
744 Takizawa, P.A., Sil, A., Swedlow, J.R., Herskowitz, I., and Vale, R.D. (1997). Actin-dependent
745 localization of an RNA encoding a cell-fate determinant in yeast. Nature 389, 90-93.
746 Teixeira, D., Sheth, U., Valencia-Sanchez, M.A., Brengues, M., and Parker, R. (2005).
747 Processing bodies require RNA for assembly and contain nontranslating mRNAs. RNA 11, 371-
748 382.
749 Vuppalanchi, D., Coleman, J., Yoo, S., Merianda, T.T., Yadhati, A.G., Hossain, J., Blesch, A.,
750 Willis, D.E., and Twiss, J.L. (2010). Conserved 3'-untranslated region sequences direct
751 subcellular localization of chaperone protein mRNAs in neurons. The Journal of biological
752 chemistry 285, 18025-18038.

bioRxiv preprint doi: https://doi.org/10.1101/159376; this version posted July 4, 2017. The copyright holder for this preprint (which was not certified by peer review) is the author/funder, who has granted bioRxiv a license to display the preprint in perpetuity. It is made available under aCC-BY 4.0 International license.

753 Weidner, J., Wang, C., Prescianotto-Baschong, C., Estrada, A.F., and Spang, A. (2014). The
754 polysome-associated proteins Scp160 and Bfr1 prevent P body formation under normal growth
755 conditions. J Cell Sci 127, 1992-2004.
756 Weil, T.T., Parton, R.M., Herpers, B., Soetaert, J., Veenendaal, T., Xanthakis, D., Dobbie, I.M.,
757 Halstead, J.M., Hayashi, R., Rabouille, C., et al. (2012). Drosophila patterning is established by
758 differential association of mRNAs with P bodies. Nat Cell Biol 14, 1305-1313.
759 Wickens, M., Bernstein, D.S., Kimble, J., and Parker, R. (2002). A PUF family portrait: 3'UTR
760 regulation as a way of life. Trends in genetics : TIG 18, 150-157.
761 Wilinski, D., Qiu, C., Lapointe, C.P., Nevil, M., Campbell, Z.T., Tanaka Hall, T.M., and Wickens,
762 M. (2015). RNA regulatory networks diversified through curvature of the PUF protein scaffold.
763 Nat Commun 6, 8213.
764 Wilson, W.A., Wang, Z., and Roach, P.J. (2002). Analysis of respiratory mutants reveals new
765 aspects of the control of glycogen accumulation by the cyclin-dependent protein kinase Pho85p.
766 FEBS letters 515, 104-108.
767 Wu, J., Zhang, N., Hayes, A., Panoutsopoulou, K., and Oliver, S.G. (2004). Global analysis of
768 nutrient control of gene expression in Saccharomyces cerevisiae during growth and starvation.
769 Proceedings of the National Academy of Sciences of the United States of America 101, 3148-
770 3153.
771 Zeiner, G.M., Cleary, M.D., Fouts, A.E., Meiring, C.D., Mocarski, E.S., and Boothroyd, J.C.
772 (2008). RNA analysis by biosynthetic tagging using 4-thiouracil and uracil
773 phosphoribosyltransferase. Methods in molecular biology 419, 135-146.
774 Zenklusen, D., Larson, D.R., and Singer, R.H. (2008). Single-RNA counting reveals alternative
775 modes of gene expression in yeast. Nat Struct Mol Biol 15, 1263-1271.
776 Zenklusen, D., Wells, A.L., Condeelis, J.S., and Singer, R.H. (2007). Imaging real-time gene
777 expression in living yeast. CSH Protoc 2007, pdb prot4870.

bioRxiv preprint doi: https://doi.org/10.1101/159376; this version posted July 4, 2017. The copyright holder for this preprint (which was not certified by peer review) is the author/funder, who has granted bioRxiv a license to display the preprint in perpetuity. It is made available under aCC-BY 4.0 International license.

778